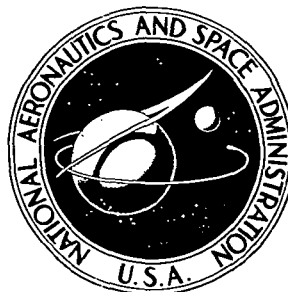**NASA CONTRACTOR REPORT**

NASA CR-2422

NASA CR-2422

THE EFFECT OF YTTRIUM AND THORIUM ON THE OXIDATION BEHAVIOR OF Ni-Cr-A*l* ALLOYS

by Arun Kumar, M. Nasrallah, and D. L. Douglass

Prepared by
UNIVERSITY OF CALIFORNIA
Los Angeles, Calif.
for Ames Research Center

NATIONAL AERONAUTICS AND SPACE ADMINISTRATION • WASHINGTON, D. C. • MAY 1974

1. Report No. NASA CR-2422	2. Government Accession No.	3. Recipient's Catalog No.
4. Title and Subtitle THE EFFECT OF YTTRIUM AND THORIUM ON THE OXIDATION BEHAVIOR OF Ni-Cr-Aℓ ALLOYS		5. Report Date MAY 1974
		6. Performing Organization Code
7. Author(s) Arun Kumar, M. Nasrallah and D. L. Douglass		8. Performing Organization Report No.
		10. Work Unit No.
9. Performing Organization Name and Address University of California School of Engineering & Applied Science Los Angeles, California		11. Contract or Grant No. NGR 05-007-352
		13. Type of Report and Period Covered
12. Sponsoring Agency Name and Address National Aeronautics & Space Administration Washington, D.C. 20546		Interim Summary Report
		14. Sponsoring Agency Code

15. Supplementary Notes

16. Abstract

The effect of quaternary additions of 0.5% Y, 0.5 and 1.0% Th to a base alloy of Ni-10Cr-5Aℓ on the oxidation behavior and mechanism was studied during oxidation in air over the range of 1000 to 1200°C. The presence of yttrium decreased the oxidation kinetics slightly, whereas, the addition of thorium caused a slight increase. Oxide scale adherence was markedly improved by the addition of the quaternary elements.

Although a number of oxides formed on yttrium-containing alloys, quantitative X-ray diffraction clearly showed that the rate-controlling step was the diffusion of aluminum through short-circuit paths in a thin layer of alumina that formed parabolically with time. Mixed oxides containing both aluminum and yttrium formed by the reaction of Y_2O_3 to form $YAℓO_3$ initally, and $Y_3Aℓ_5O_{12}$ (YAG) after longer times. Although the scale adherence of the yttrium-containing alloy was considerably better than the base alloys, spalling did occur that was attributed to the formation of the voluminous YAG particles which grew in a "mushroom"-like manner, lifting the protective scale off the substrate locally. The YAG particles formed primarily at grain boundaries in the substrate in which the yttrium originally existed as YNi_9. This intermetallic compound reacted to form Y_2O_3, liberating metallic nickel that subsequently reacted to form NiO and/or $NiAℓ_2O_4$ spinel. The Y_2O_3 reacted with aluminum to ultimately form the YAG "mushrooms."

Thorium did not form any mixed oxides; the only oxide involving thorium was ThO_2, which existed as small particles at the oxide-metal interface. A highly beneficial effect of the thoria particles in reducing film spalling was observed.

Scale spalling in the base alloy was attributed to void formation at the oxide-metal interface, the voids forming by condensation of excess vacancies from the Kirkendall effect associated with slow back-diffusion of nickel into the substrate as aluminum was preferentially oxidized and diffused rapidly outward. The mechanism of improved scale adherence in the quaternary alloys was the elimination of voids by annihilation of the Kirkendall vacancies at vacancy sinks introduced by the non-coherent interfaces between yttrium and thorium-containing intermetallics and/or oxides.

17. Key Words (Suggested by Author(s)) Kinetics, Diffusion, Oxide Scale, Defect Structure, Internal Oxidation, Scale Adherence	18. Distribution Statement UNCLASSIFIED-UNLIMITED CAT. 17

19. Security Classif. (of this report) UNCLASSIFIED	20. Security Classif. (of this page) UNCLASSIFIED	21. No. of Pages 42	22. Price* $3.25

*For sale by the National Technical Information Service, Springfield, Virginia 22151

Page Intentionally Left Blank

TABLE OF CONTENTS

ABSTRACT

The effect of quaternary additions of 0.5%Y, 0.5 and 1.0%Th to a base alloy of Ni-10Cr-5Al on the oxidation behavior and mechanism was studied during oxidation in air over the range of 1000 to 1200°C. The presence of yttrium decreased the oxidation kinetics slightly, whereas, the addition of thorium caused a slight increase. Oxide scale adherence was markedly improved by the addition of the quaternary elements.

Although a number of oxides formed on yttrium-containing alloys, quantitative X-ray diffraction clearly showed that the rate-controlling step was the diffusion of aluminum through short-circuit paths in a thin layer of alumina that formed parabolically with time. Mixed oxides containing both aluminum and yttrium formed by the reaction of Y_2O_3 to form $YAlO_3$ initially, and $Y_3Al_5O_{12}$ (YAG) after longer times. Although the scale adherence of the yttrium-containing alloy was considerably better than the base alloys, spalling did occur that was attributed to the formation of the voluminous YAG particles which grew in a "mushroom"-like manner, lifting the protective scale off the substrate locally. The YAG particles formed primarily at grain boundaries in the substrate in which the yttrium originally existed as YNi_9. This intermetallic compound reacted to form Y_2O_3, liberating metallic nickel that subsequently reacted to form NiO and/or $NiAl_2O_4$ spinel. The Y_2O_3 reacted with aluminum to ultimately form the YAG "mushrooms."

Thorium did not form any mixed oxides; the only oxide involving thorium was ThO_2, which existed as small particles at the oxide-metal interface. A highly beneficial effect of the thoria particles in reducing film spalling was observed.

Scale spalling in the base alloy was attributed to void formation at the oxide-metal interface, the voids forming by condensation of excess vacancies from the Kirkendall effect associated with slow back-diffusion of nickel into the substrate as aluminum was preferentially oxidized and diffused rapidly outward. The mechanism of improved scale adherence in the quaternary alloys was the elimination of voids by annihilation of the Kirkendall vacancies at vacancy sinks introduced by the non-coherent interfaces between yttrium and thorium-containing intermetallics and/or oxides.

INTRODUCTION

Low strength and poor oxidation resistance limit the use of nickel-base alloys for high temperature structural applications in the range of 1000 to 1200°C. The strength of these alloys decreases markedly with increasing temperature. The lack of strength has been overcome by dispersion hardening the materials with thoria particles, producing thoria-dispersed-nickel (TD-Ni) and thoria-dispersed nichrome (TD-Ni-20Cr). However, the oxidation resistance of these materials has still not proven adequate for their use as structural components at high temperatures. It was of interest, therefore, to improve the oxidation resistance of Ni-Cr alloys with ternary and quaternary additions, so that more oxidation resistant matrices can be obtained, to which dispersoids can be added for high-temperature strength.

The initial oxidation of "Nichrome"-type alloys (Ni-20Cr) occurs with the formation of a NiO layer by outward nickel cation diffusion, enriching the substrate with chromium. Eventually, the chromium reacts with NiO and/or dissolved oxygen to form Cr_2O_3 beneath the NiO layer. The composite layer of NiO and Cr_2O_3 is thermodynamically unstable at high temperatures and reacts to form the spinel $NiCr_2O_4$. Thus, after a sufficiently long time, the scale will consist of an outer layer of spinel and an inner layer of Cr_2O_3.[1,2] If the chromium content is increased above 25%, only Cr_2O_3 forms as the outer layer. When Cr_2O_3 is the outer layer, it oxidizes to CrO_3 at very high temperatures (above 1000°C). CrO_3 is a gas and offers no protection. Thus, in order to achieve high-temperature oxidation resistance, it is necessary to form an oxide scale which is not volatile and which has a low defect concentration.

An example of an oxide that fulfills these requirements is Al_2O_3, which forms during the oxidation of binary alloys containing aluminum, if the aluminum content is high enough. The addition of aluminum to nickel should, in principle, result in alloys that could be oxidized to form Al_2O_3 scales, the oxidation behavior being analogous to that of Ni-Cr alloys. However, the Al_2O_3 film of Ni-Al alloys spalls readily,[3] but if some critical amount of chromium exists in the alloy, the spalling tendency is reduced.

The amount of aluminum required to form Al_2O_3 depends on the chromium content of the alloys as shown in Fig. 1, which is an "oxide-map" of the Ni-Cr-Al system[4] at 1000°C. It has been shown that Ni-Cr-Al alloys generally exhibit excellent oxidation resistance.[5,6] Kvernes and Kofstad[5] found that the best alloy composition was Ni-9.3Cr-5.8Al for optimum iso-thermal oxidation resistance.

It has been found also that small additions of reactive metals, e.g., Y, Th, Ca, Ce, Sm, etc. are very beneficial and provide good oxidation resistance and/or scale adherence. Kvernes and Kofstad[5] added up to 0.7 w/o yttrium to a Ni-9Cr-6Al alloy and found improved scale adherence and a reduction in the oxidation rate. Yttrium existed in the grain boundaries of the alloy in the form of Ni-Y intermetallics which oxidized preferentially, giving rise to a "keying-on" effect of the oxide scale. There was no yttrium found in the scales. This observation is not in agreement with that of Kuenzly and Douglass, who observed an enrichment only at the inner portion of the oxide formed at 1200°C on a Ni-20Cr-1Y alloy.

This study involved the determination of the optimum composition of a Ni-Cr-Al ternary alloy for both oxidation resistance and the least tendency for spalling of the films. Small amounts of yttrium and thorium were added to this Ni-Cr-Al ternary alloy, and the mechanism of oxidation and the oxide scale adherence was determined.

EXPERIMENTAL PROCEDURES

Materials and Sample Preparation

The following metals were used for melting of alloys: Ni--99.99%, Cr--99.99%, Al--99.999%, Y--99.9%, and Th--99.5%. The charges were pickled in order to remove any surface films that might exist, rinsed, and ultrasonically cleaned in acetone. The weighed charges (total of about 100 grams) were arc-melted in argon with a non-consumable electrode. The argon was gettered with a titanium button that was melted, thereby removing any residual oxygen or nitrogen. The buttons were turned over and remelted five times in order to obtain homogeneity. Melting losses
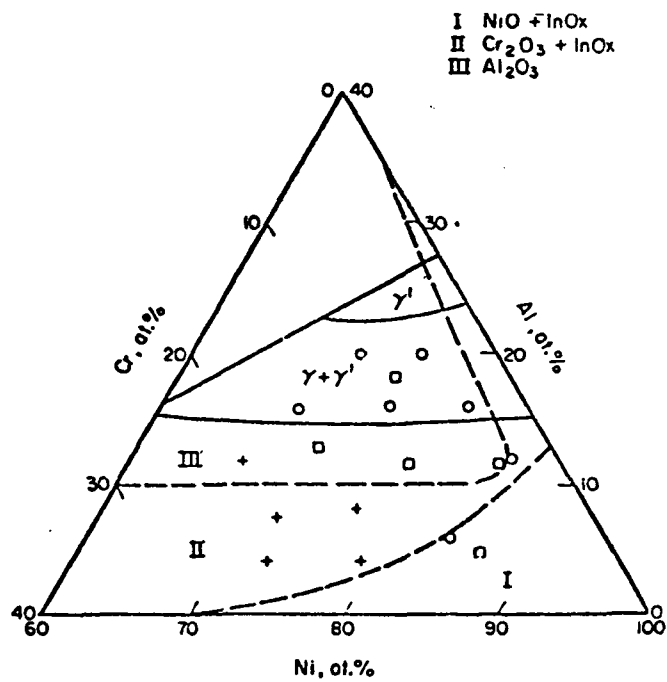
3

Fig. 1 Oxide map for the ternary system Ni-Cr-Aℓ at 1000°C.[4]

4

were about 0.1% or less, and thus the compositions were taken as the nominal ones.

The buttons were cut into slices about 0.1 inch thick with a metallographic cutoff wheel. The slices were cleaned with acetone and given a homogenization treatment for 24 hrs. at 1000°C in vacuum (10^{-6} torr). The slices were ground through 4/0 emery paper and vacuum-annealed for 30 mins. at 900°C.

Oxidation Tests

Thermal gravimetric analyses were performed in a Harrop Unit that required about 20 mins. to reach a temperature of 1200°C. The weight gain increased rapidly with time during heat up, commencing at a temperature of about 900°C. This problem was eliminated by preoxidizing the sample in another furnace by rapidly immersing the samples into the furnace which was already at the desired temperature. This method would produce those oxides which were characteristic of the actual oxidizing temperature rather than those formed upon heating. All the samples with yttrium and thorium additions were initially weighed and preoxidized at the temperature of oxidation for one-half hour. No spalling was observed during cooling to room temperature. These samples were subsequently reweighed and introduced in a Harrop thermal gravimetric unit which was then heated to the temperature of oxidation. No changes were observed during heating when the samples were preoxidized. Samples of the base alloy Ni-10Cr-5Aℓ, spalled after the half-hour preoxidation at 1200 and 1150°C, hence the Harrop unit was modified for direct immersion of the sample into the hot-zone of the furnace at the oxidation temperature.

The quarternary alloys containing Y and Th exhibited no spalling either at temperature during the test or during the cool-down after oxidation.

Various pretreatments were studied which were shown to have an effect on the oxidation kinetics. On the basis of these tests a standard pretreatment of vacuum-annealing for 30 mins. at 900°C was adopted.

X-Ray Diffraction Studies

The oxides formed during oxidation were identified by X-ray diffraction studies made on the "in-situ" scales and spalled oxides. A Phillips

Norelco diffractometer was used with nickel-filtered copper radiation.

The transient stage of oxidation was studied by immersing the alloy samples directly into the hot-zone of the furnace for varying times. The development of various oxidation products and the sequence of their formation were studied by X-ray diffraction.

Scanning Electron Microscopy

The scanning electron microscope (SEM) was used to study the surface features of the oxides, and the mode of fracture of the spalled oxides. Identification of the phases present was performed with an X-ray image and microprobe attachment to the SEM using line-scans for various elements.

Metallographic Examination

The oxidized samples were vapor-deposited with silver, and then a heavy coating of copper was applied electrolytically. A thin vapor coating of silver was necessary for copper plating. The copper coating was applied in order to keep the oxide film from fracturing during the metallographic preparation. A Bausch and Lomb metallograph was used to examine the samples.

RESULTS

Oxidation Behavior of Ternary Ni-Cr-Aℓ Alloys

The first tests were conducted on ternary Ni-Cr-Aℓ alloys in order to determine the best alloy to which quaternary additions could be made. Selection of compositions was based on data in the literature[4,5,8,9] regarding oxidation rates, film spalling, and fabricability. Three compositions were initially selected, shown in Fig. 2, and tested. The results of these tests were used to select additional compositions, also shown in Fig. 2 along with Kvernes and Kofstad's alloys.[5]

The kinetics of oxidation are shown in Fig. 3 as a log-log plot of weight gain vs. time. The log-log plots were used for convenience in covering several decades of time. The alloys showed two distinct classifications: Group 1 (Ni-12Cr-3Aℓ and Ni-5Cr-5Aℓ) oxidized much more rapidly than Group 2. The Ni-5Cr-5Aℓ alloy exhibited variable behavior, some samples exhibiting Group-2 behavior.

All of the ternary alloys except one, Ni-12Cr-3Aℓ, exhibited extensive spalling of their oxides during cooling from the oxidation temperature.
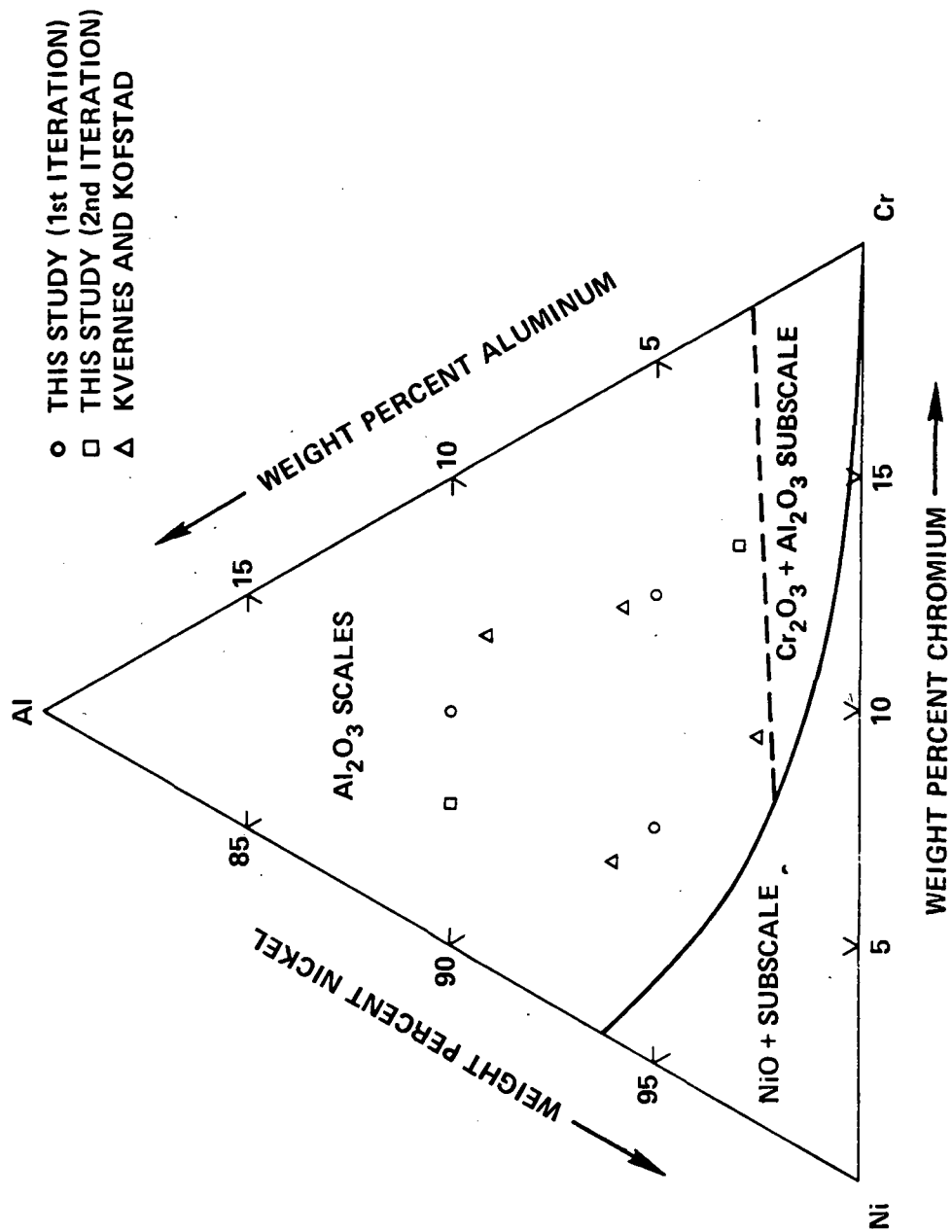
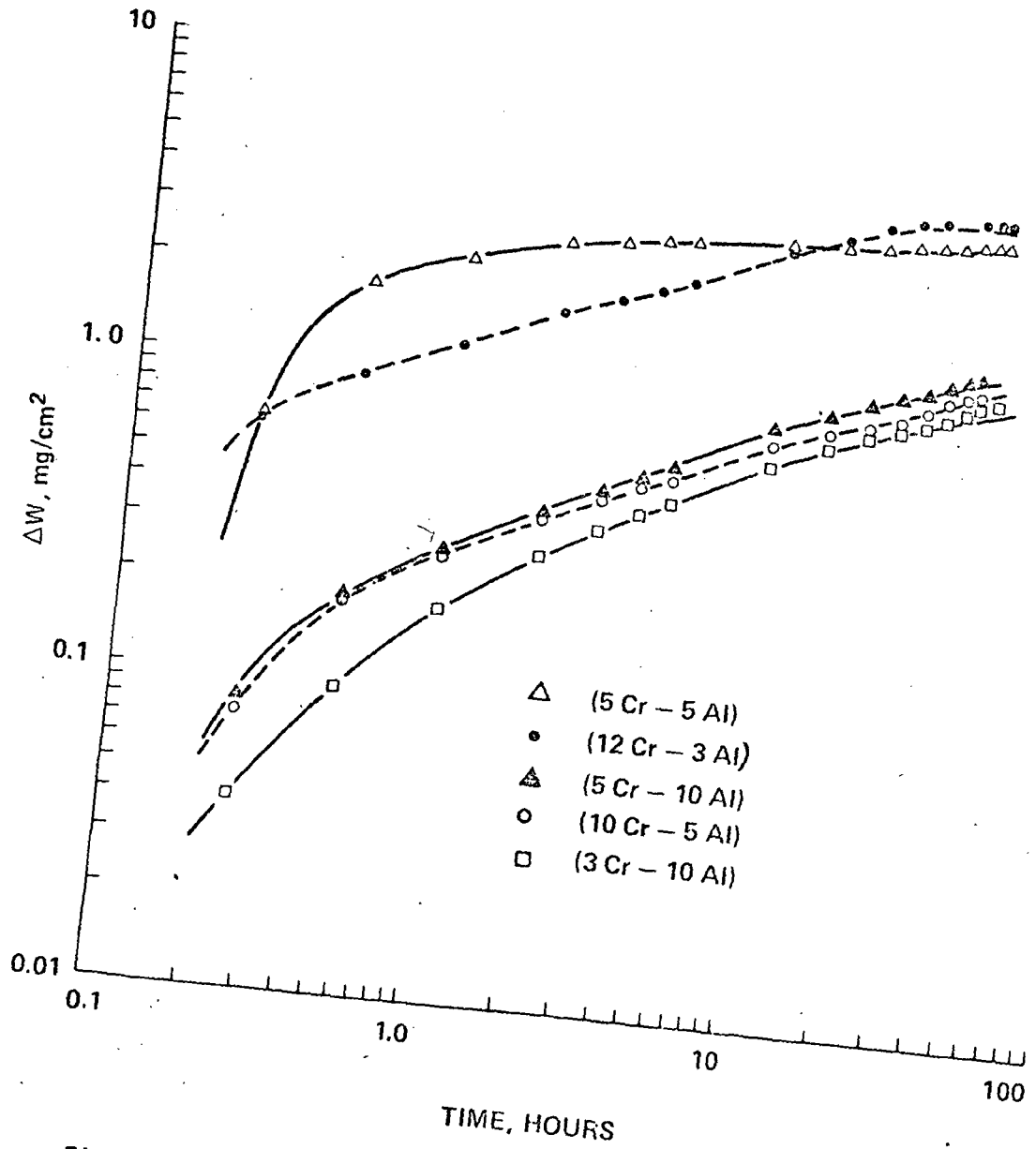Fig. 2 Oxide "map" at 1200°C showing alloy compositions.

o THIS STUDY (1st ITERATION)
□ THIS STUDY (2nd ITERATION)
△ KVERNES AND KOFSTAD

WEIGHT PERCENT ALUMINUM

WEIGHT PERCENT NICKEL

WEIGHT PERCENT CHROMIUM

Al$_2$O$_3$ SCALES

Cr$_2$O$_3$ + Al$_2$O$_3$ SUBSCALE

NiO + SUBSCALE

Al

Cr

Ni

Fig. 3 Oxidation kinetics of Ni-Cr-Aℓ alloys in Air at 1200°C.

8

Effect of Quaternary Additions on Oxidation Behavior

Two of the ternary alloys were selected as base compositions to which 0.5%Y was added. The first, Ni-10Cr-5Aℓ, was near optimum with respect to oxidation behavior, and the second, Ni-12Cr-3Aℓ, was the only alloy that could be cold-rolled. This alloy exhibited less than optimum oxidation resistance, but it was thought that yttrium might markedly improve the oxidation and yet not impair the fabricability. As will be shown, the oxidation behavior was improved with the yttrium addition, but the fabricability was decreased. Thorium was added to the Ni-10Cr-5Aℓ alloy. Both yttrium and thorium improve the scale adherence of these alloys. Three alloys, Ni-10Cr-5Aℓ-0.5Y, Ni-10Cr-5Aℓ-0.5Th and Ni-10Cr-5Aℓ-1Th were oxidized at 1000, 1100, 1150 and 1200°C and intensively studied.

The effect of yttrium on the oxidation kinetics is shown in Fig. 4. Little difference, probably within experimental scatter, was noted for the Ni-10Cr-5Aℓ alloy with and without yttrium, but a noticeable decrease in oxidation rate occurred upon the addition of 0.5%Y to Ni-12Cr-3Aℓ.

The effect of temperature on the oxidation behavior of Ni-10Cr-5Aℓ, Ni-10Cr-5Aℓ-0.5Y, Ni-10Cr-5Aℓ-0.5Th, and Ni-10Cr-5Aℓ-1Th is shown in Figs. 5-8, and the corresponding parabolic plots are shown in Figs. 9-12, respectively. The base alloy Ni-10Cr-5Aℓ had a variable oxidation behavior at 1000°C, and so the results are not reported. For the alloys with Y and Th additions, however, reproducible results were obtained from 1000 to 1200°C. All the thermogravimetric data were obtained on at least two samples.

None of the alloys followed a strict parabolic time dependence as noted by the continuously decreasing slope of parabolic plots. The parabolic plots indicate that the overall reaction is diffusion-controlled after extended oxidation. However, because more than one oxide forms, no physical interpretation should be associated with the apparent long-time parabolic behavior; the parabolic rate constants were determined for comparative purposes, as shown in Fig. 13, an Arrhenius plot of the rate constants. This plot also includes data for pure nickel and a Ni-25w/oAℓ which forms
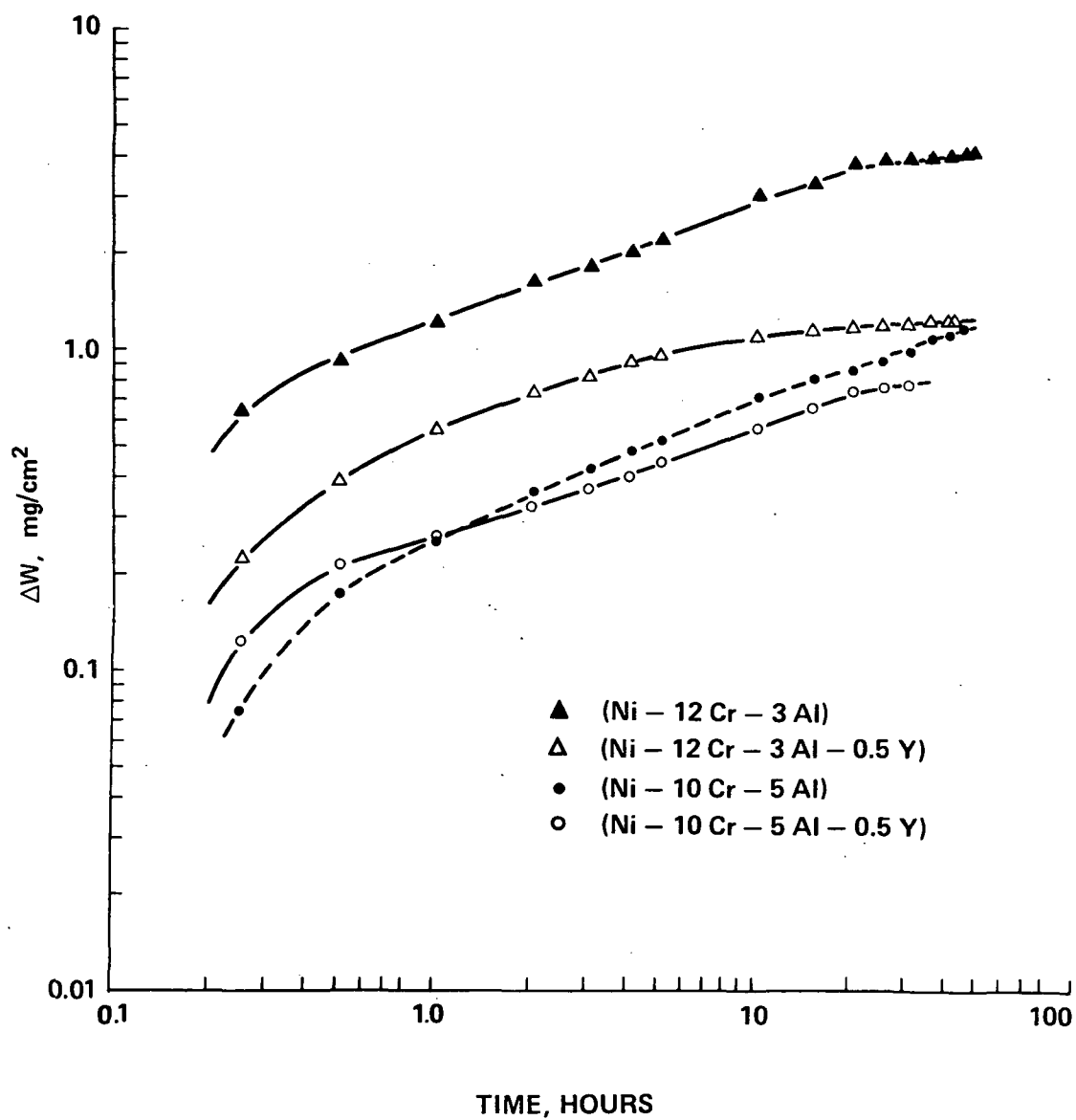
Fig. 4   Effect of yttrium on the oxidation kinetics of two Ni-Cr-Al alloys at 1200°C in air.
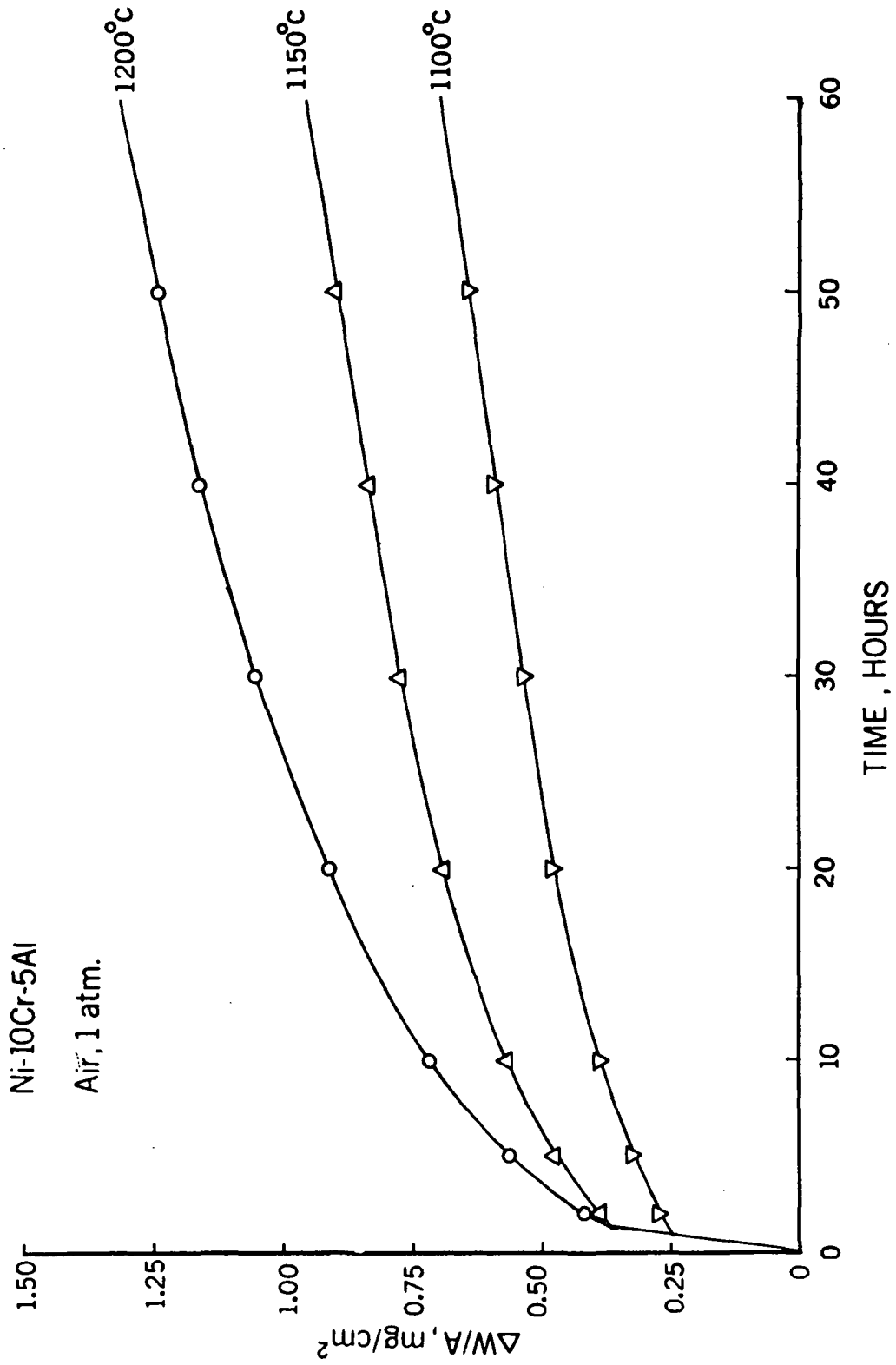
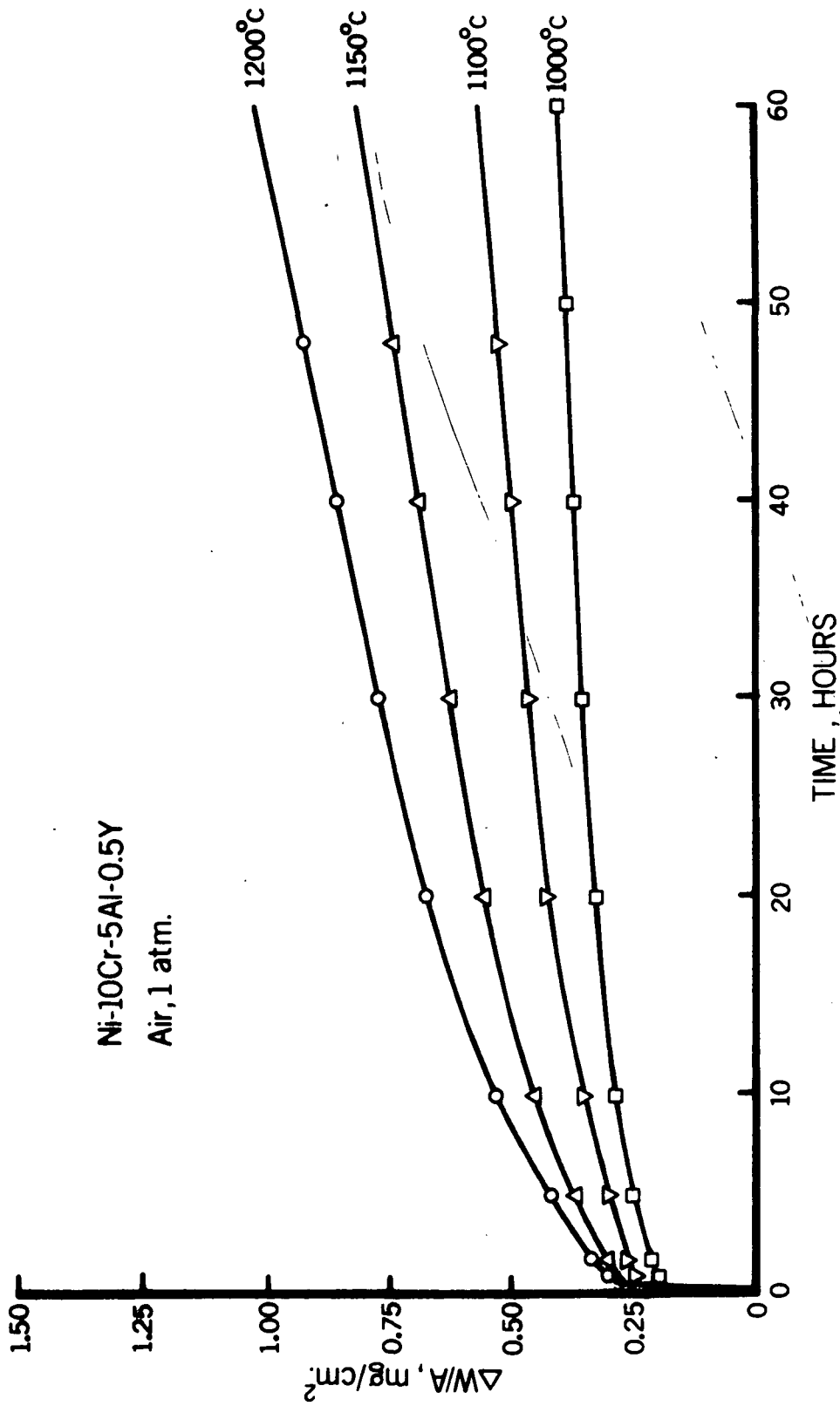Fig. 5   Effect of temperature on the oxidation behavior of Ni-10Cr-5Aℓ.

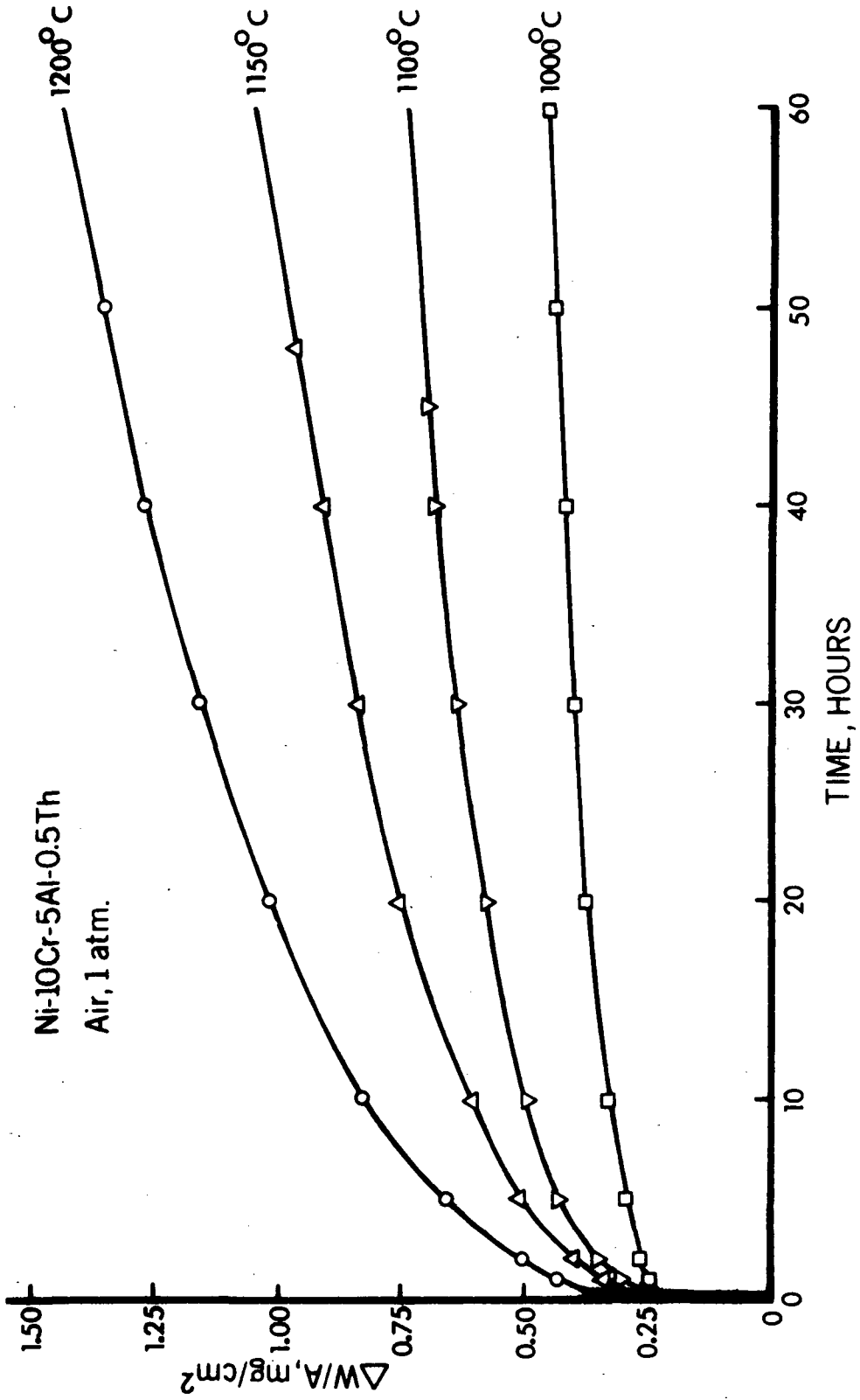Fig. 6 Effect of temperature on the oxidation behavior of Ni-10Cr-5Aℓ-0.5Y

12

Fig. 7   Effect of temperature on the oxidation behavior of Ni-10Cr-5Aℓ-0.5Th
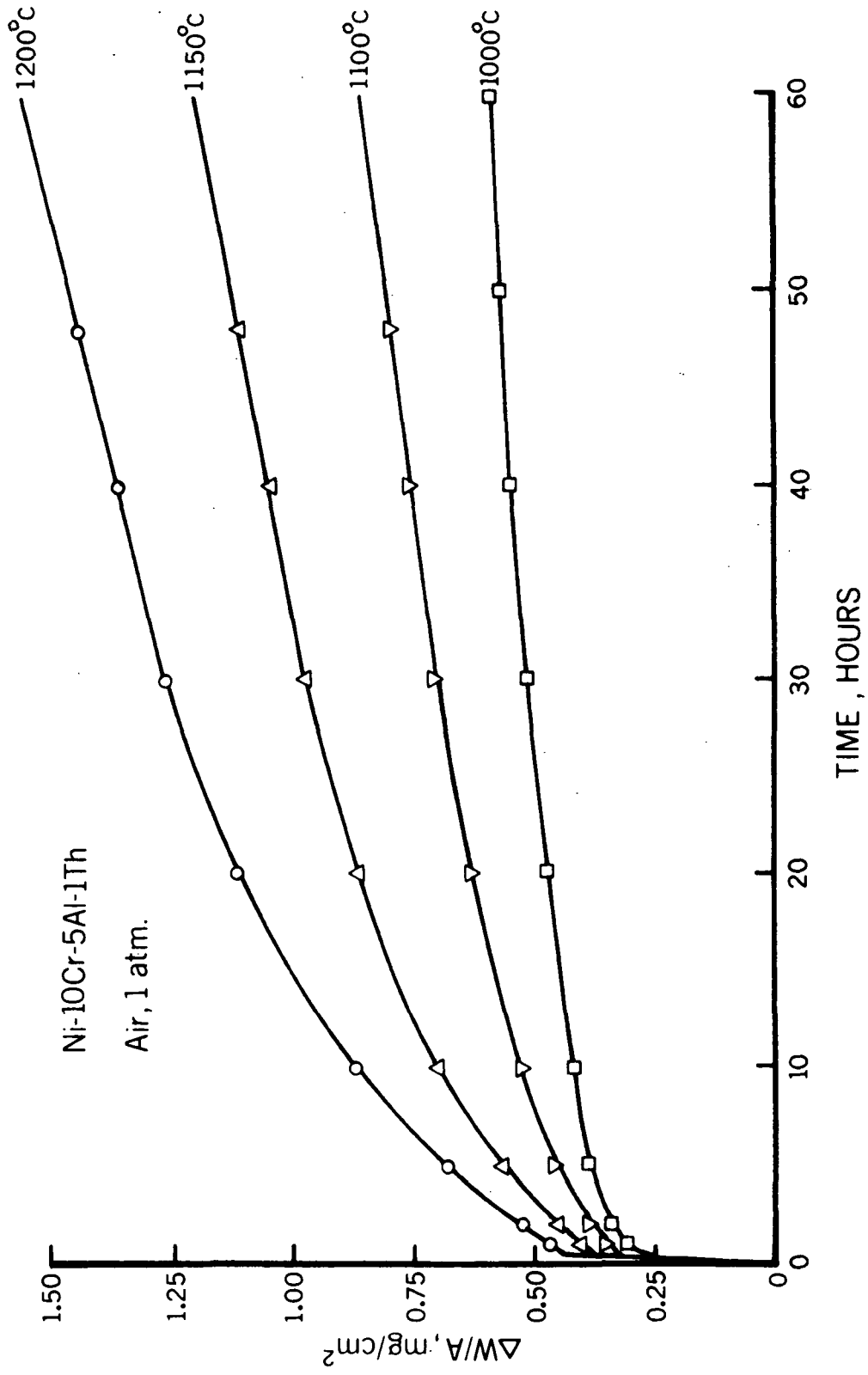
13

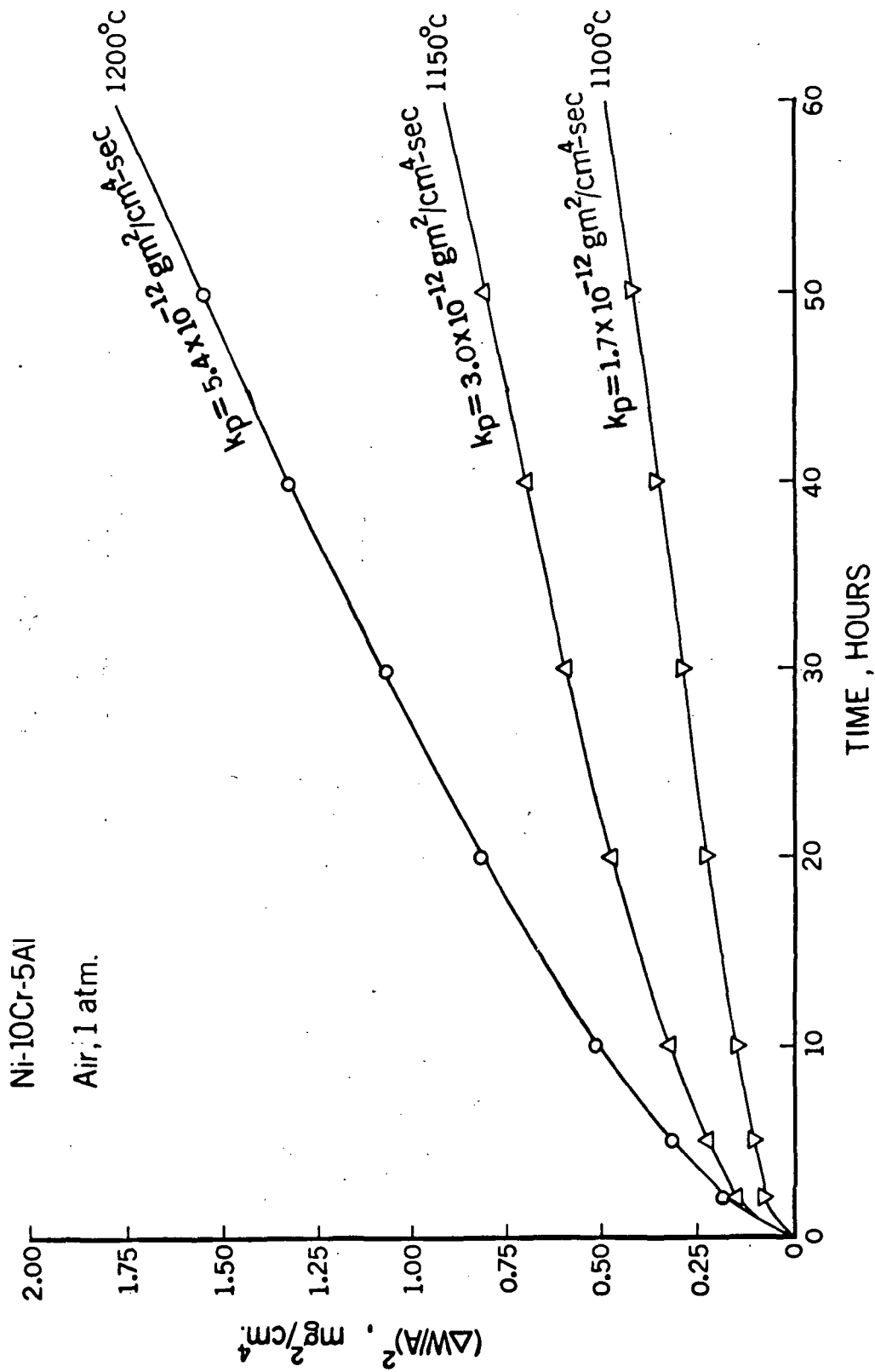Fig. 8   Effect of temperature on the oxidation behavior of Ni-10Cr-5Aℓ-1Th

14

Fig. 9 Parabolic Plot for the oxidation of Ni-10Cr-5Aℓ from 1100-1200°C in atm. air.

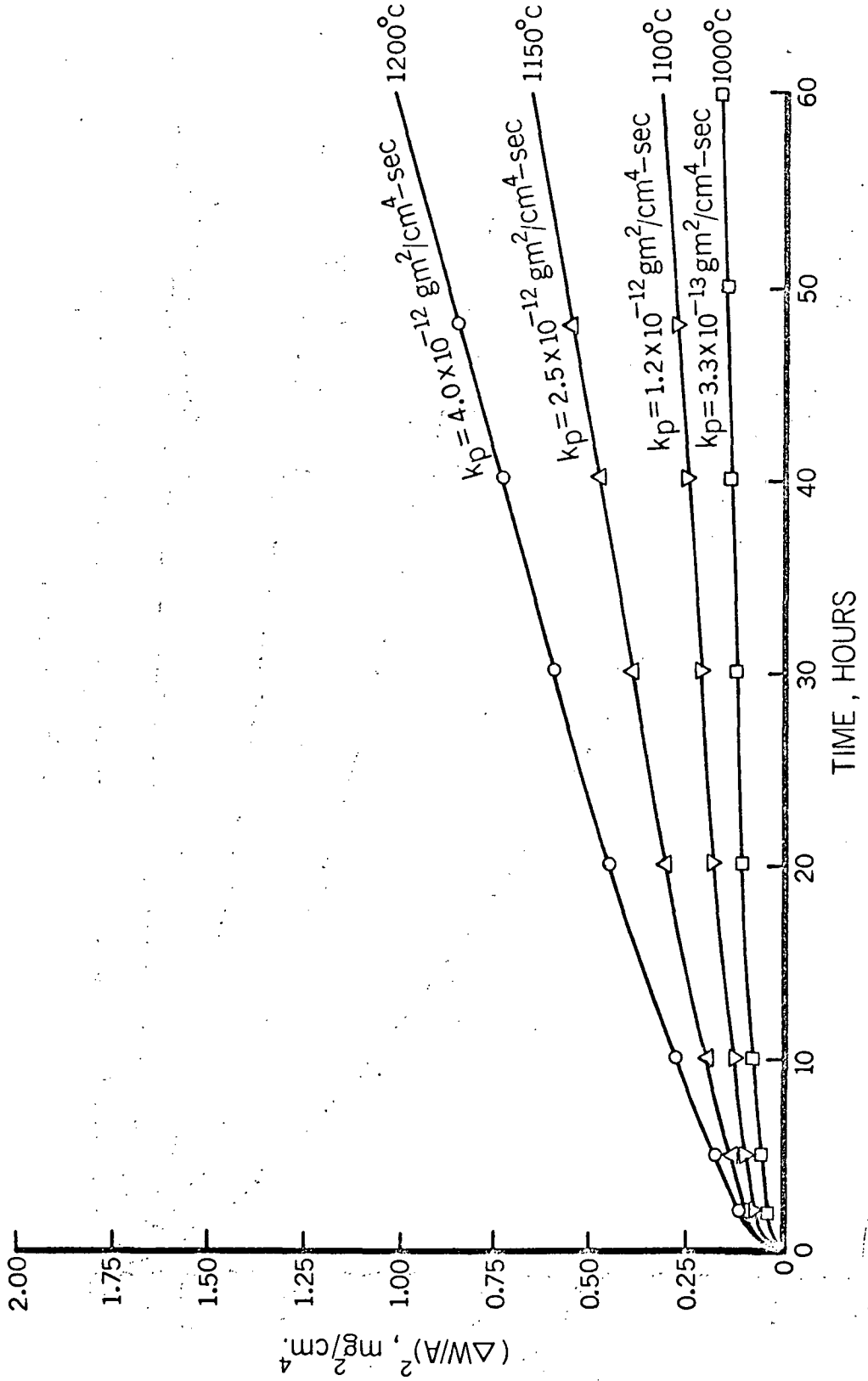Fig. 10 Parabolic plot for the oxidation of Ni-10Cr-5Aℓ-0.5Y from 1000-1200°C in 1 atm air.
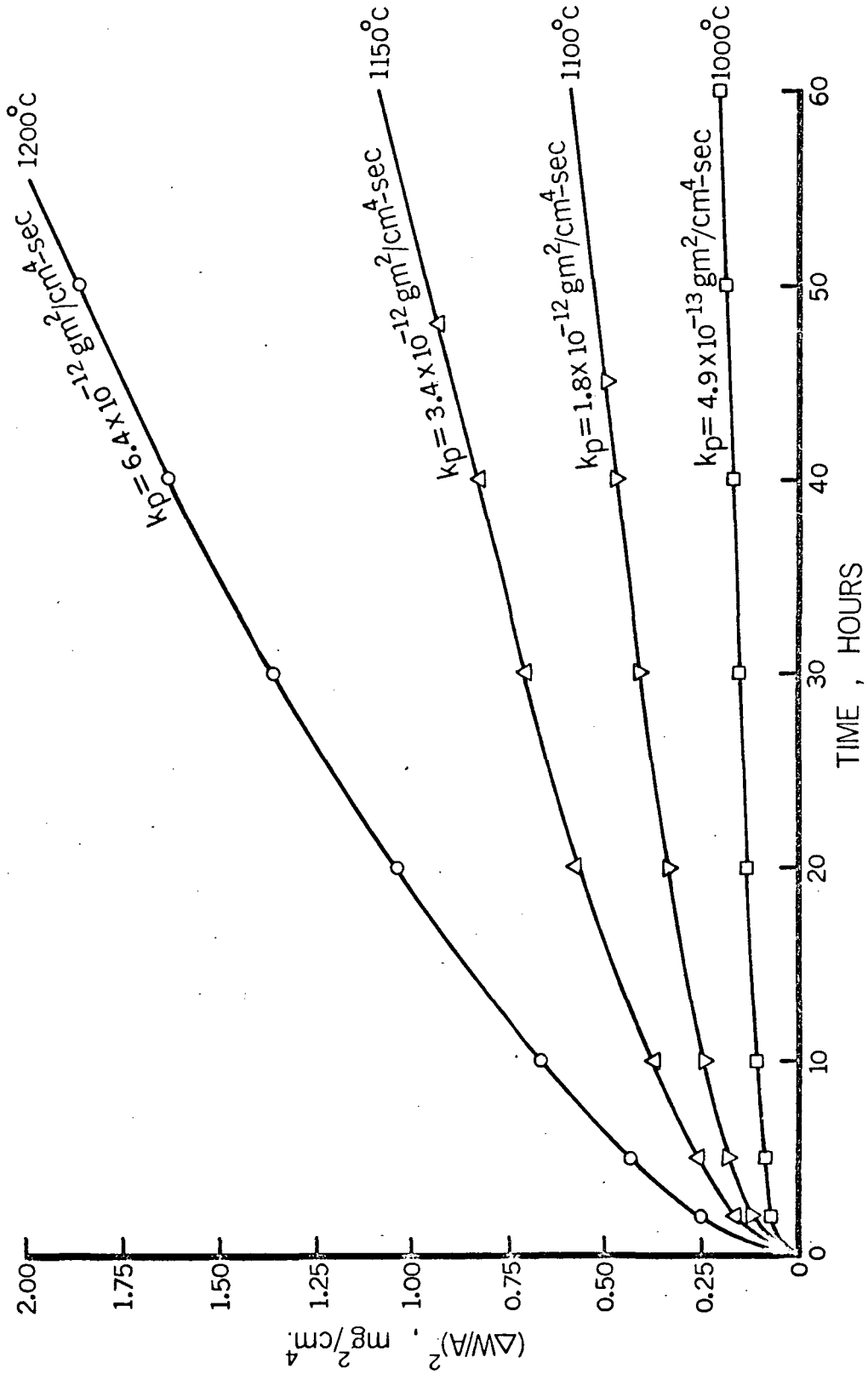
16

Fig. 11 Parabolic plot for the oxidation of Ni-10Cr-5Aℓ-0.5Th from 1000-1200°C in 1 atm. air.
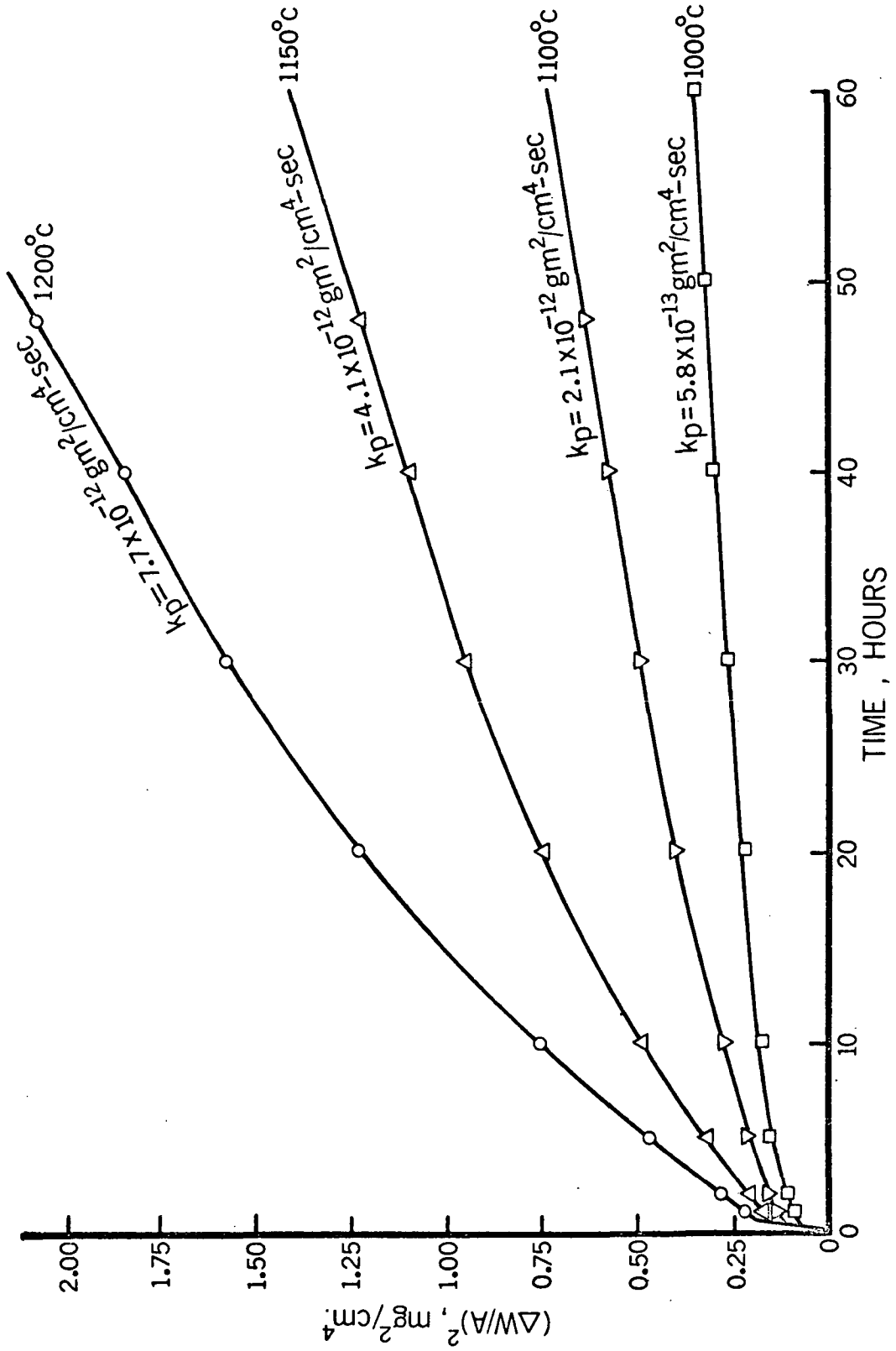
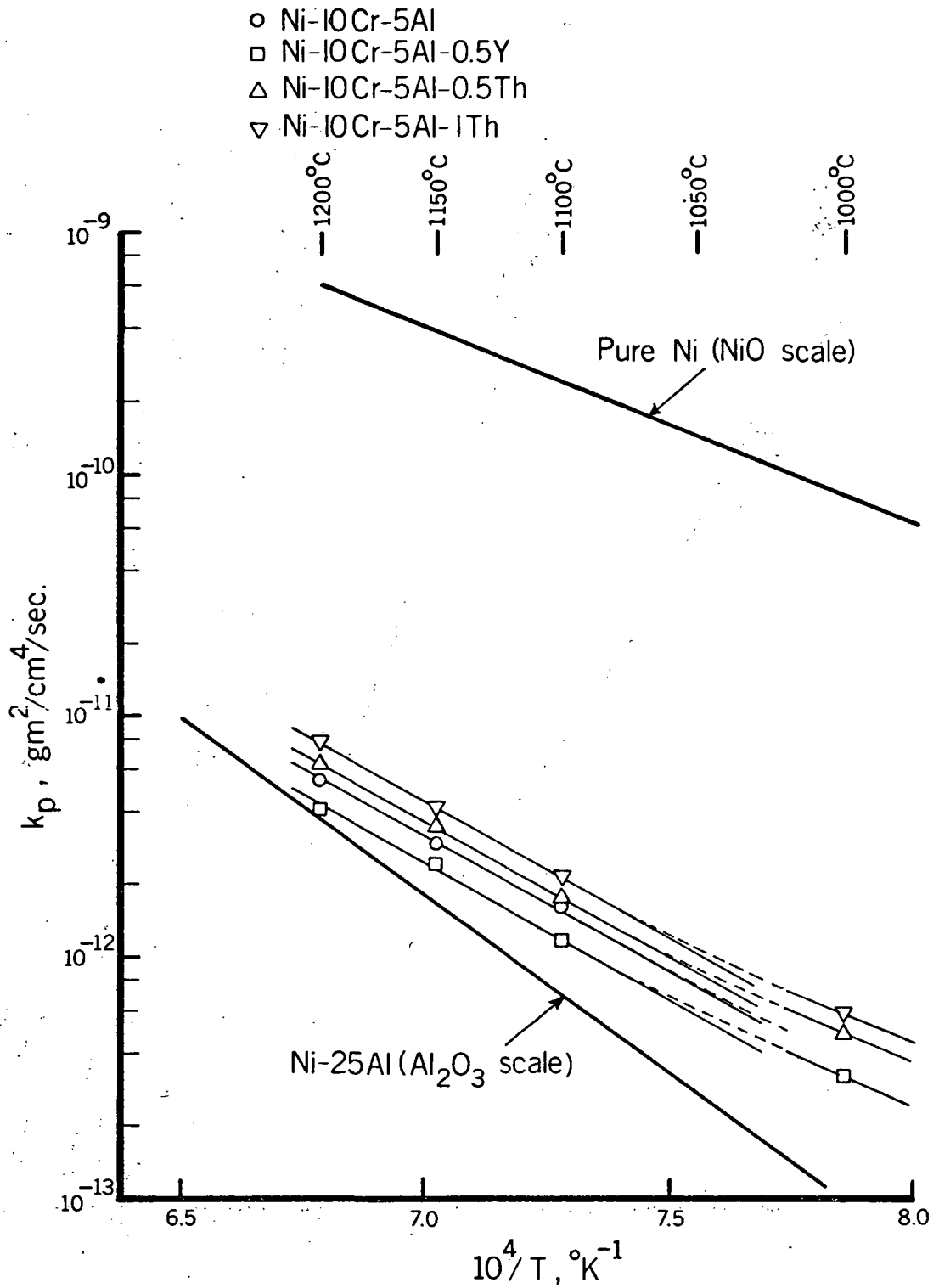Fig. 12 Parabolic plot for the oxidation of Ni-10Cr-5Aℓ-1Th from 1000-1200°C in 1 atm. air.

18

Fig. 13 Arrhenius plot for various alloys showing temperature dependence.

α-Al_2O_3 upon oxidation. It can be seen that at 1000°C, the data points deviate from a straight line. This is due to the formation of NiO, the main oxide on these alloys at lower temperatures. The activation energies for all alloys were almost the same, e.g., approximately 50 Kcal/mole. It is also evident that thorium increases the oxidation rate of Ni-10Cr-5Al slightly, whereas, yttrium caused a slight decrease in the oxidation rate.

X-ray diffraction analyses were made on "in-situ" oxide scales,and whenever possible, on the spalled oxides. A summary of the oxide phases present and their relative amounts is given in Table I for various alloys oxidized in static air at 1 atm. at the temperature and time indicated. It is evident that for the Ni-10Cr-5Al alloy with yttrium or thorium additions, the amount of α-Al_2O_3 and $NiAl_2O_4$ increases while the amount of NiO decreases with an increase in the oxidation temperature. In addition to α-Al_2O_3, $NiAl_2O_4$ and NiO, the Ni-10Cr-5Al-0.5Y alloy also shows a weak peak of Y_2O_3 at 1000°C, $YAlO_3$ from 1100 to 1200°C, and $Y_3Al_5O_{12}$ at 1150 and 1200°C. The Ni-10Cr-5Al-0.5Th and Ni-10Cr-5Al-1Th alloys exhibited a weak peak for ThO_2; no complex oxides containing thorium were detected.

The development of oxides on Ni-10Cr-5Al-0.5Y at 1200°C was studied as a function of time using quantitative X-ray diffractometry. Fig. 14 shows the transient stages of oxide scale development for periods ranging from 5 to 400 mins. It can be seen that NiO nucleates and grows very rapidly while α-Al_2O_3 and $NiAl_2O_4$ form discrete nuclei within the first few minutes. Very small amounts of Cr_2O_3 and $NiCr_2O_4$ were also detected after 5 mins. At the same time, Ni-Y intermetallics are converted to Y_2O_3, which subsequently disappears after about 100 mins., combining with α-Al_2O_3 to form the double oxide, $YAlO_3$. With increasing time, α-Al_2O_3 grows and more α-Al_2O_3 reacts with $YAlO_3$ to form $Y_3Al_5O_{12}$ (garnet structure). A diffuse peak for the Y-Al garnet (YAG) appears after approximately 200 mins. The appearance of the YAG corresponds to the onset of limited spalling of the outer oxide layer, which can be seen also by the increase in the intensity of the substrate reflection. An analysis of the diffracted intensities from various oxides revealed that the thickness of the α-Al_2O_3 layer increases parabolically with time.

20

TABLE I

SUMMARY OF X-RAY ANALYSES OF OXIDES FORMED IN AIR.

ALLOY	OXIDATION TEMP.	OXIDATION TIME	X-RAY INTENSITY OF "IN-SITU" OXIDES			SPALLED OXIDES
			STRONG	MEDIUM	WEAK	
Ni-5Cr-5Al	1200°C	24 hrs.	α-Al_2O_3 + $NiAl_2O_4$	NiO	-	α-Al_2O_3+$NiAl_2O_4$
Ni-5Cr-10Al	1200°C	24 hrs.	α-Al_2O_3	-	$NiAl_2O_4$	α-Al_2O_3
Ni-10Cr-5Al	1200°C	25 hrs.	α-Al_2O_3	$NiAl_2O_4$	-	α-Al_2O_3+$NiAl_2O_4$
Ni-3Cr-10Al	1200°C	50 hrs.	NiO	-	-	α-Al_2O_3+$NiAl_2O_4$
Ni-12Cr-3Al	1200°C	48 hrs.	NiO + Cr_2O_3	$NiCr_2O_4$	α-Al_2O_3+$NiAl_2O_4$	Not analyzed
Ni-12Cr-3Al-0.5Y	1200°C	42 hrs.	NiO+$NiCr_2O_4$+Cr_2O_3	-	α-Al_2O_3+$NiAl_2O_4$	Not analyzed
Ni-10Cr-5Al-0.5Th*	1200°C	50 hrs.	α-Al_2O_3 + $NiAl_2O_4$	-	ThO_2	No spalling
Ni-10Cr-5Al-0.5Th*	1150°C	48 hrs.	α-Al_2O_3 + $NiAl_2O_4$	-	NiO + ThO_2	No spalling
Ni-10Cr-5Al-0.5Th*	1100°C	45 hrs.	-	NiO + α-Al_2O_3 + $NiAl_2O_4$	ThO_2	No spalling
Ni-10Cr-5Al-0.5Th	1000°C	62 hrs.	NiO	-	α-Al_2O_3+$NiAl_2O_4$+ThO_2	No spalling
Ni-10Cr-5Al-1Th*	1200°C	48 hrs.	α-Al_2O_3 + $NiAl_2O_4$	-	ThO_2	No spalling
Ni-10Cr-5Al-1Th*	1150°C	48 hrs.	α-Al_2O_3 + $NiAl_2O_4$	-	NiO + ThO_2	No spalling
Ni-10Cr-5Al-1Th*	1100°C	48 hrs.	-	NiO + α-Al_2O_3 + $NiAl_2O_4$	ThO_2	No spalling
Ni-10Cr-5Al-1Th*	1000°C	72 hrs.	NiO	-	α-Al_2O_3+$NiAl_2O_4$+ThO_2	No spalling
Ni-10Cr-5Al-0.5Y*	1200°C	48 hrs.	α-Al_2O_3 + $NiAl_2O_4$	-	$YAlO_3$ + $Y_3Al_5O_{12}$	Not analyzed
Ni-10Cr-5Al-0.5Y*	1150°C	48 hrs.	α-Al_2O_3 + $NiAl_2O_4$	-	NiO+$YAlO_3$+$Y_3Al_5O_{12}$	No spalling
Ni-10Cr-5Al-0.5Y*	1100°C	48 hrs.	-	NiO + α-Al_2O_3 + $NiAl_2O_4$	$YAlO_3$	No spalling
Ni-10Cr-5Al-0.5Y*	1000°C	72 hrs.	NiO	-	α-Al_2O_3+$NiAl_2O_4$+Y_2O_3	No spalling

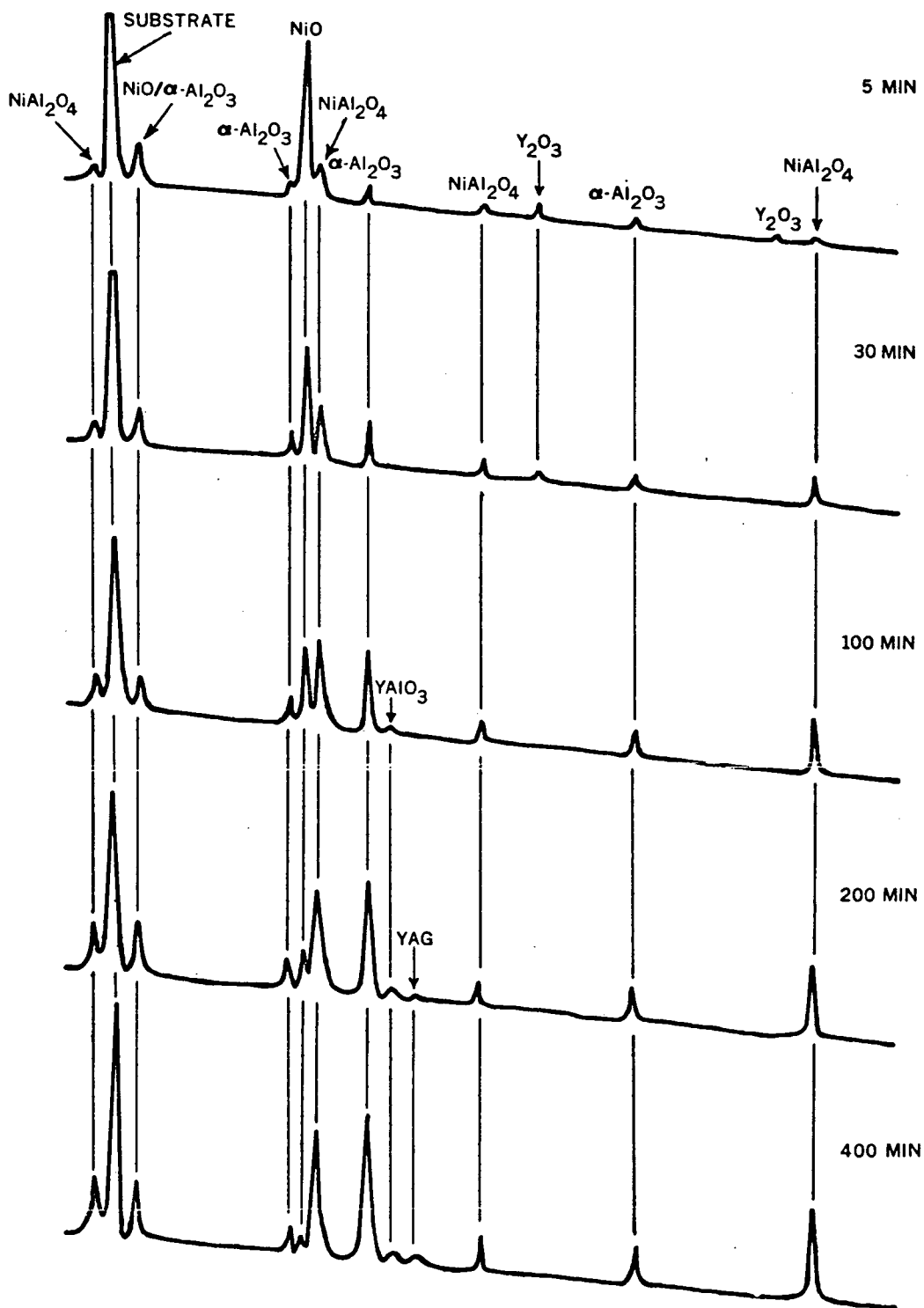*Preoxidized for one-half hour at the temperature of oxidation.

Fig. 14   X-ray diffractometer traces of the oxide scale development
          on Ni-10Cr-5Aℓ-0.5Y at 1200°C.

Fig. 15 is a plot of log peak intensity vs. log time for various oxides. The intensities were obtained from the diffractometer traces by slow scanning at 1/8° per min. Since the integral breadth indicated very little or no strain and/or particle-size broadening, peak intensities were used instead of integrated intensities. NiO decreases with increasing oxidation time, whereas $NiAl_2O_4$ increases initially and decrease subsequently at extended times. This is because NiO reacts with $\alpha-Al_2O_3$ to form $NiAl_2O_4$ via a solid-state reaction; thus, when a continuous layer of $\alpha-Al_2O_3$ is formed beneath NiO, the only NiO available for this reaction is that which formed during the initial stages of oxidation, e.g., on the outside. The amount of $NiAl_2O_4$ increases while the reaction is taking place but then decreases as the NiO is being used up and no more NiO is available for the reaction. Some Cr_2O_3, which formed initially, evaporates via the formation of CrO_3 according to the following reaction:

$$Cr_2O_3 + \frac{3}{2}O_2(g) \longrightarrow 2CrO_3(g)\uparrow$$
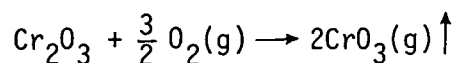
This reaction is significant above 1000°C and thus no Cr_2O_3 is detected on any of these alloys after extended oxidation. Some $NiCr_2O_4$ is formed by the solid-state reaction of Cr_2O_3 and NiO.

Spalled oxide from Ni-10Cr-5Al-0.5Y oxidized at 1200°C for four days reveals the presence of YAG particles in the detached $\alpha-Al_2O_3$ layer. After spalling had taken place, the substrate showed some YAG and $YAlO_3$ particles in the $\alpha-Al_2O_3$ layer still attached to the alloy. The structure of oxide scales formed on Ni-10Cr-5Al-0.5Y and Ni-10Cr-5Al-1Th is shown in Figs. 16 and 17, respectively. At 1200 and 1150°C, an outer scale of $NiAl_2O_4$ and an inner scale of $\alpha-Al_2O_3$ formed. At 1100 and 1000°C, some unreacted NiO formed the outermost layer, and thus a three-layer scale was observed. These results are in agreement with the X-ray diffraction data in Table I.

The surface morphology of the structure of the spalled oxide on Ni-10Cr-5Al after 30 min. exposure at 1200°C is shown in Fig. 18. The oxide islands remaining on the surface were characterized by the electron microprobe and were found to be $\alpha-Al_2O_3$ along with some small areas of $NiAl_2O_4$.
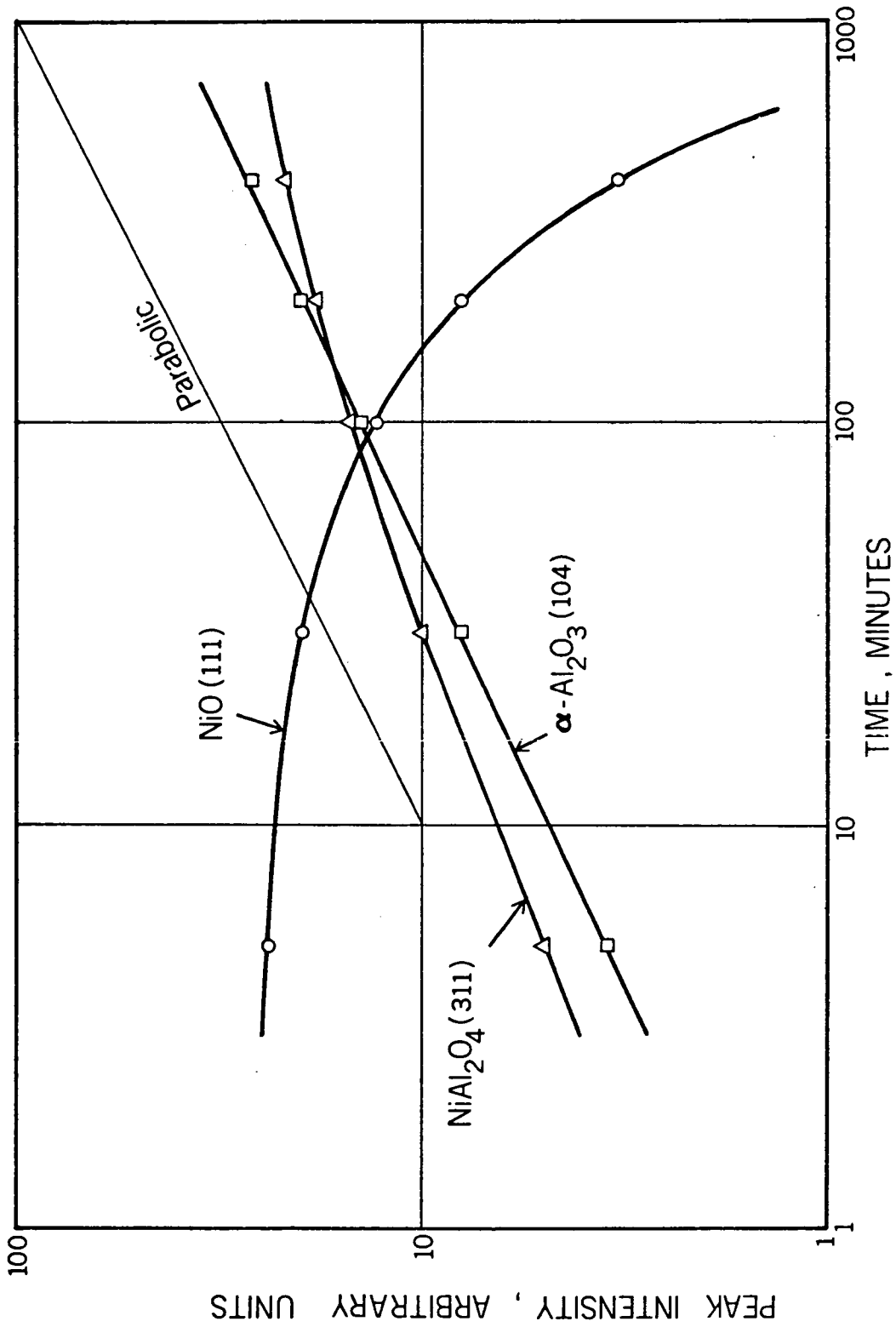
23

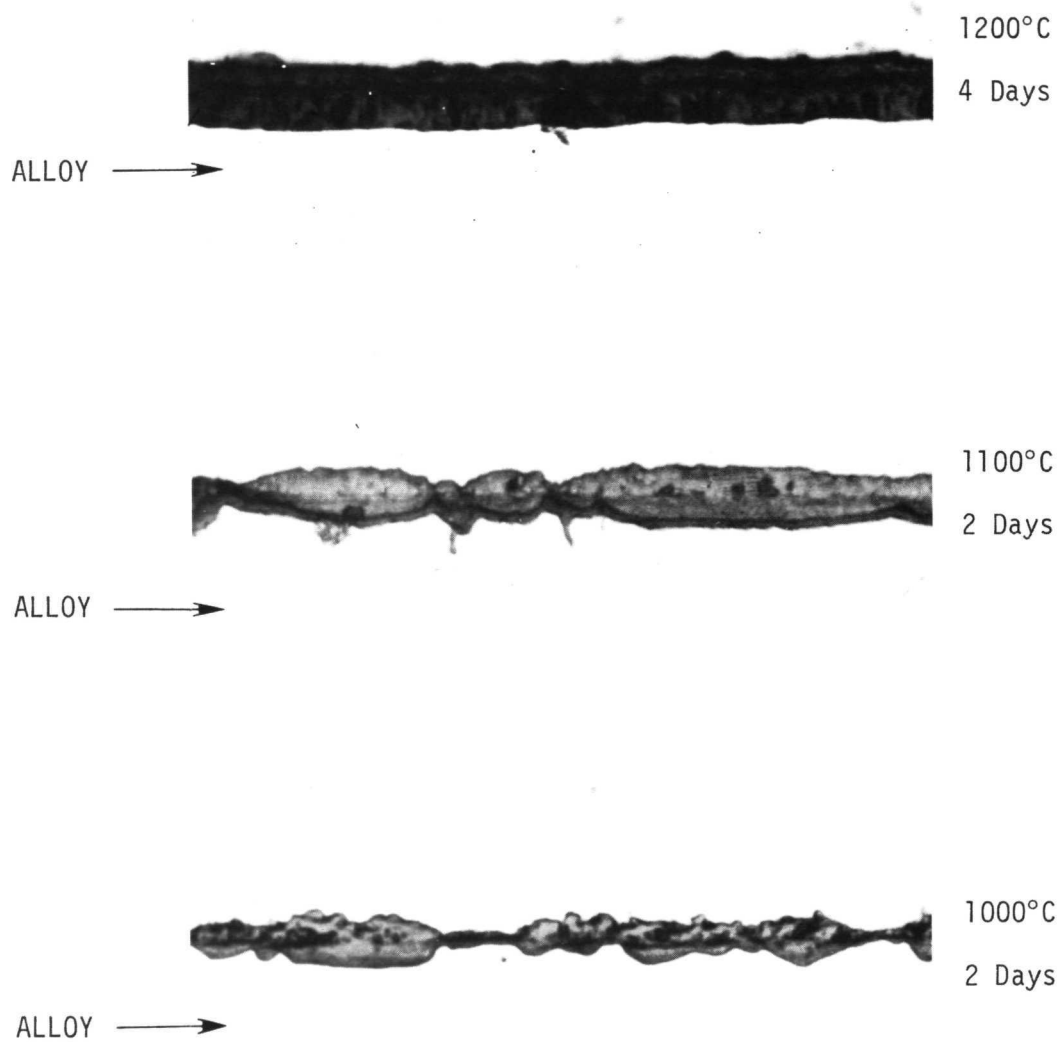Fig. 15 X-ray diffraction intensities during the transient oxidation of Ni-10Cr-5Aℓ-0.5Y at 1200°C in 1 atm. Air.

24

ALLOY ⟶   1200°C
                4 Days

ALLOY ⟶   1100°C
                2 Days

ALLOY ⟶   1000°C
                2 Days

Fig. 16 Structure of scales formed on Ni-10Cr-5Aℓ-0.5Y at various
         temperatures. 1000X

ALLOY ⟶

1200°C
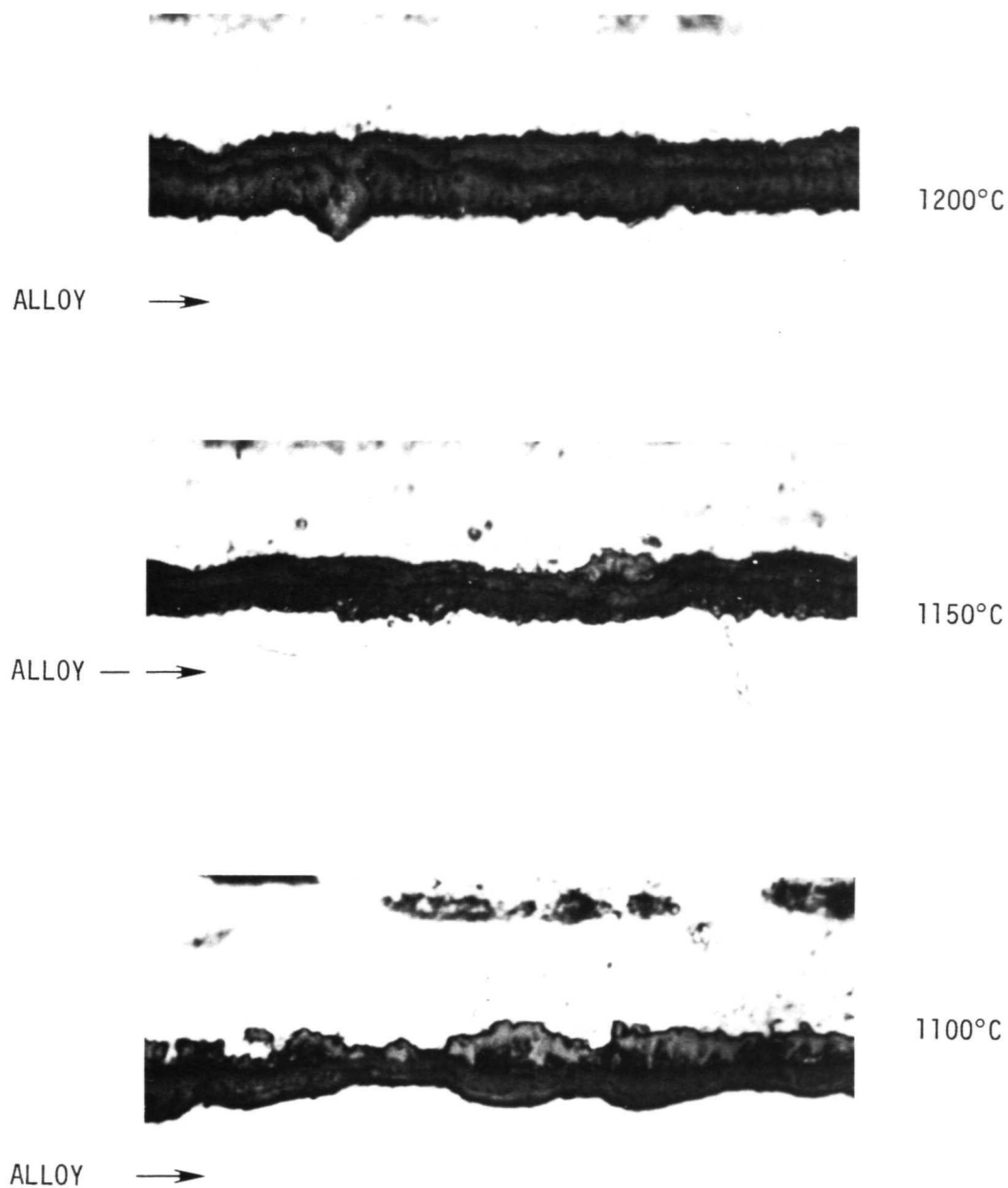
ALLOY — ⟶

1150°C

ALLOY ⟶

1100°C

Fig. 17 Structure of scales formed on Ni-10Cr-5Aℓ-Th oxidized for
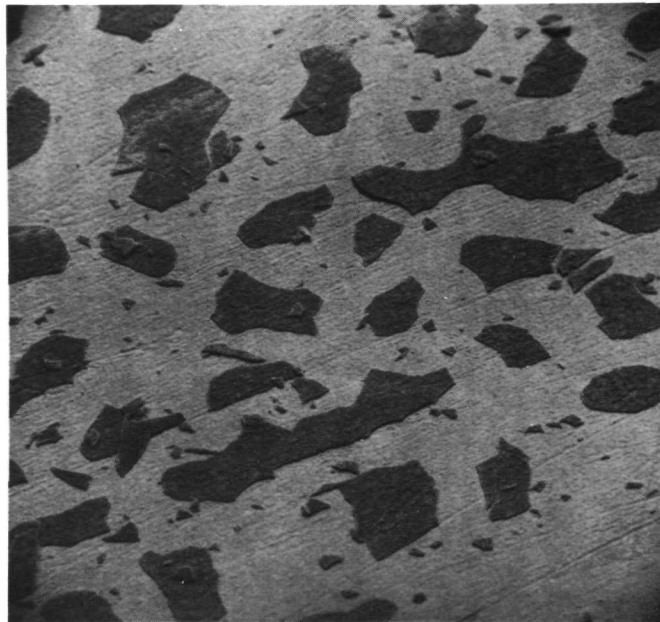2 days at various temperatures. 1400X

26

Fig. 18 Scanning electron micrograph showing spalled oxide on Ni-10Cr-5Aℓ after 30 minutes at 1200°C. 165X

A sample of Ni-10Cr-5Aℓ-1Th was immersed directly at 1200°C for one
week in air. Very limited spalling of the oxide occurred upon cooling.
A typical spalled area is shown in an optical micrograph in Fig. 19. The
ThO_2 particles can be seen embedded on the surface of the substrate, below
the outer oxide layer. Some ThO_2 particles also appear to have been pulled
out, along with the spalled oxide. The same area was also examined with
the scanning electron microscope, as shown in Fig. 20. The thoria particles
were about 20μm in diameter.

The amount of spalling on the Y-containing alloy was much less than on
the base alloy, Ni-10Cr-5Aℓ, after one week of oxidation at 1200°C, as
noted in the scanning electron micrographs in Fig. 21. No massive, detached
oxide layers were obtained during cooling as in the case of the base alloy.
The dark network in Fig. 21-a represents areas from which oxide spalled
and overlaps many grains of the alloy. Fig. 21-b shows the unspalled
region in which the substrate grain boundaries are apparent due to the
existence there of $Y_3Aℓ_5O_{12}$. A higher magnification scanning electron
micrograph from another sample (oxidized 100 hrs. at 1200°C) is shown in
Fig. 22 in which it can be seen that a small amount of YAG existed within
the grains and was still attached to the substrate, even though some YAG
particles had fractured and were lost with the spalled oxide. Some YAG
particles and some holes, from which some particles spalled, were also
detected within the grains. The substrate surface, in general, was
observed to be free of voids even at very high magnifications.

The presence of YAG particles in the grain boundaries was due to the
high yttrium content of the substrate grain boundaries which in turn was
due to the localization of Ni-Y intermetallic compounds in the alloy grain
boundaries. In order to prove this point, etched but unoxidized samples
were examined by X-ray diffraction and the electron microprobe which re-
vealed the presence of Ni_9Y, Ni_5Y, and Ni_7Y_2. The microstructure of the
base alloy and the yttrium-containing quaternary is shown in Fig. 23.

The base alloy, Ni-10Cr-5Aℓ, showed a two-phase structure (γ+γ') at
room temperature [Fig. 22(a)]. It is interesting to note that the addition
of yttrium changed the structure of Ni-10Cr-5Aℓ. The Ni-Y intermetallics
formed preferentially at the grain boundaries, the excess aluminum being
confined to the grains. The γ-phase consists of a primary solid solution
of Cr and Aℓ in nickel and has a face-centered cubic (FCC) structure which
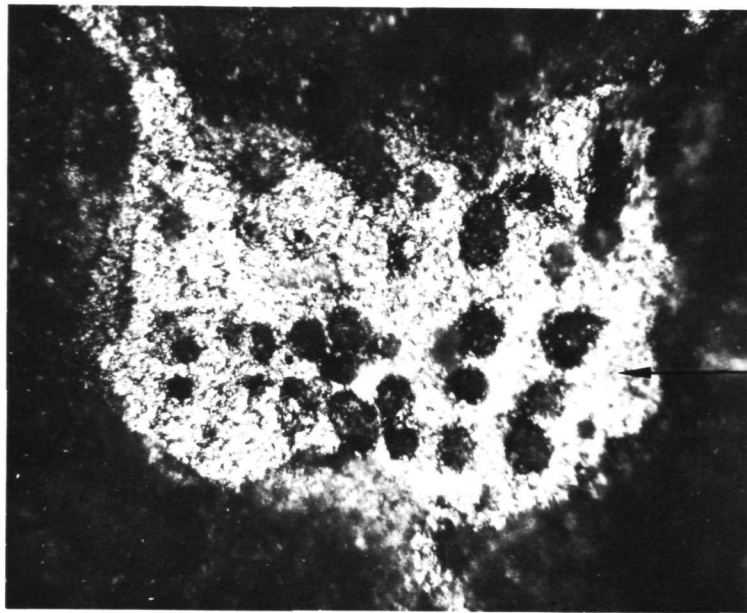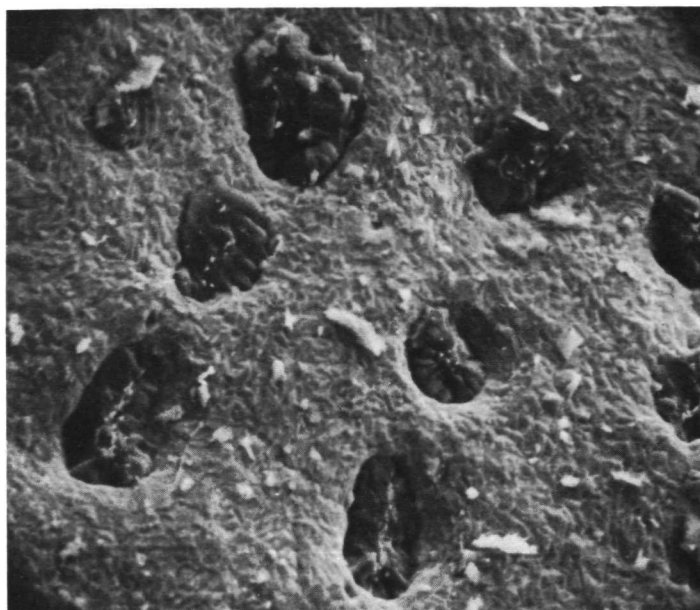
(a)   250X
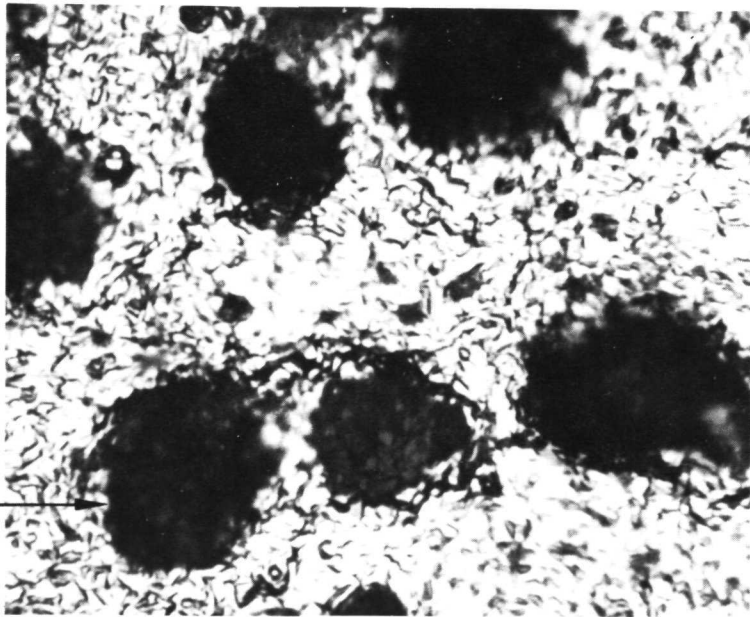
(a)   1000X

Fig. 19 Optical micrographs showing ThO_2 particles on a spalled area on Ni-10Cr-5Aℓ-1Th oxidized at 1200°C for one week.

29

(a)   1000X
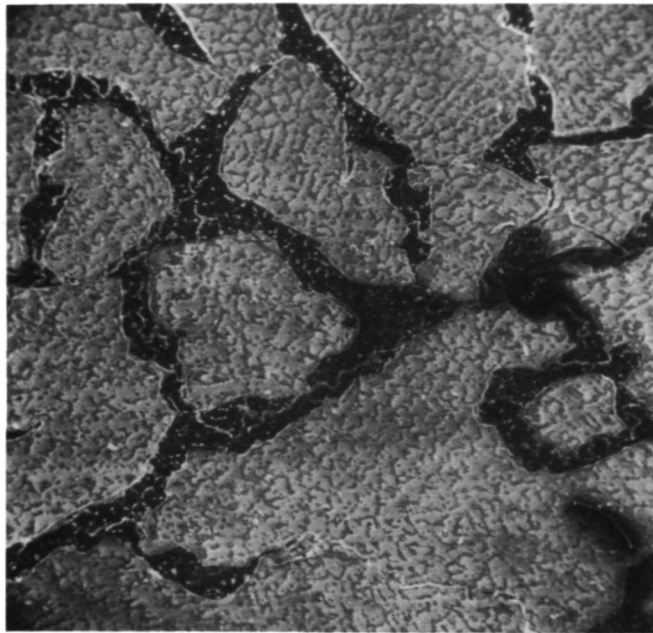
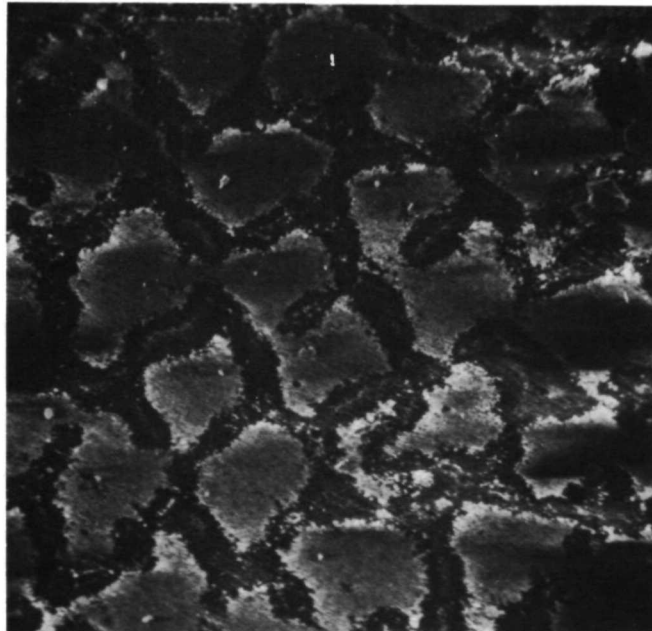(b)   2000X

Fig. 20 Scanning electron micrographs showing ThO_2 particles on a spalled area on Ni-10Cr-5Aℓ-1Th oxidized at 1200°C for one week.

(a)   40X


(b)   350X

Fig. 21   Scanning electron micrograph showing limited spalling on Ni-Cr-5Aℓ-0.5Y
          after one week of oxidation in air at 1200°C. (a) shows that the
          limited spalling overlaps many grains. (b) is an enlargement of the
          "unspalled" area showing the grain boundaries. The oxide formed over
          the substrate grains is $Aℓ_2O_3$, and the oxide formed over the grain
   boundaries is $Y_3Aℓ_5O_{12}$.
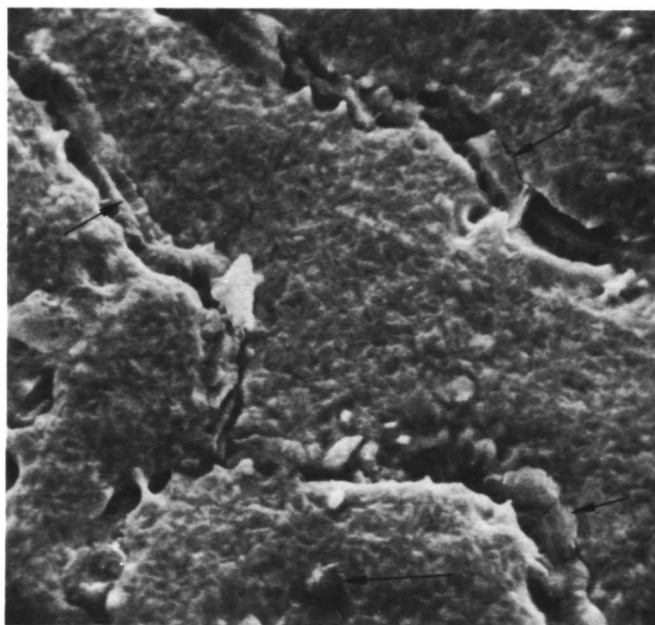
1000X

Fig. 22 Scanning electron micrograph showing typical substrate
surface after the oxide has spalled from Ni-10Cr-5Aℓ-0.5Y
after 100 hr. of oxidation in air at 1200°C. The micro-
graph shows the grain boundaries from which the yttrium-
aluminum garnet has spalled. The arrows point to particles
of yttrium-aluminum garnet which are still attached to the
substrate.

32

(a)   250X

Ni-10Cr-5Aℓ

Ni-Y inter-
metallics

(b)   200X
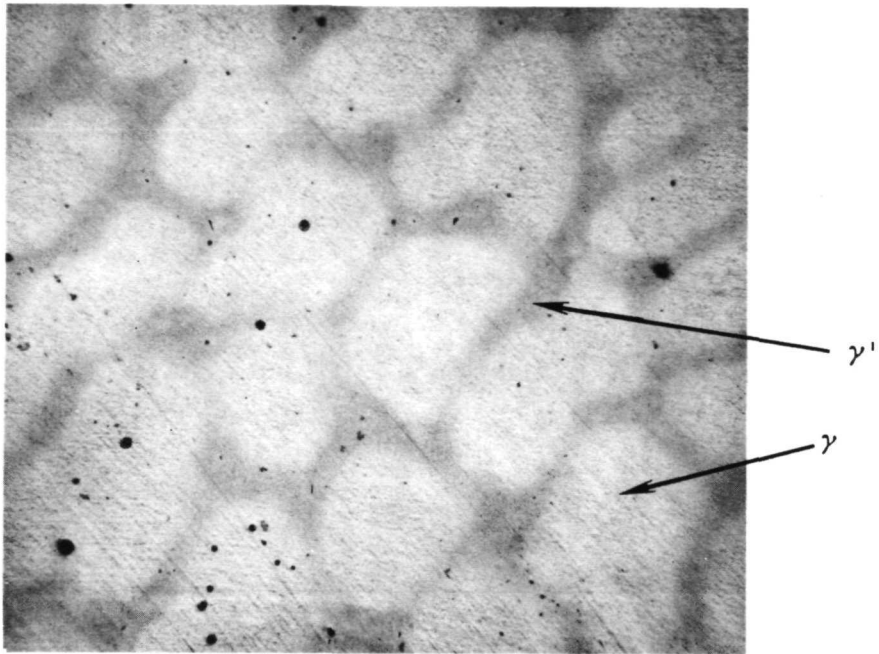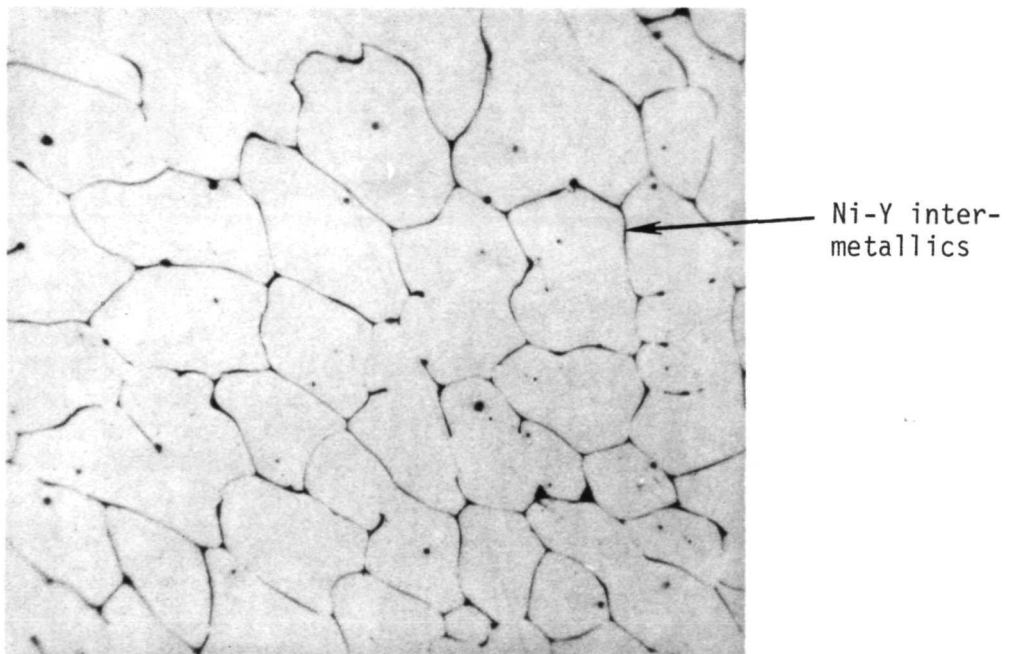
Ni-10Cr-5Aℓ-0.5Y

Fig. 23 Etched surface of unoxidized alloys.

can be ordered in the neighborhood of Ni_3Cr below 540°C. [9] The
γ-phase is based on the structure of Ni_3Al, which has an ordered FCC
lattice in which nickel atoms occupy the cube faces and aluminum and
chromium atoms occupy the cube corners. [10]

The alloys containing 0.5 and 1 w/o thorium did not contain inter-
metallics, however, a small amount of ThO_2 was detected in the surface
layers of vacuum-annealed and unoxidized alloys. The microstructure
did not reveal any grain boundary precipitates.

As described earlier, the oxide film on Ni-10Cr-5Al, without the
additions of yttrium or thorium, tended to be non-adherent. A patch of
oxide which was still adherent to the surface of Ni-10Cr-5Al after
24 hrs. of oxidation at 1200°C is shown in Fig. 24. An enlarged view
[Fig. 24(b)] shows that there were areas over which the oxide had
partially separated from the substrate.

A piece of partially detached oxide scale from Ni-10Cr-5Al after
50 hrs. oxidation at 1200°C was examined at an angle of 75° in cross-
section. The scanning micrograph is shown in Fig. 25 and shows a string
of voids formed at the bottom of the oxide at the oxide/metal interface.
These voids cause a loss of contact of the oxide, which eventually leads
to spallation of the oxide. These voids were also observed on the under-
side of the detached oxide, i.e., at the oxide/metal interface, as shown
in Fig. 26. The oxide showed a granular structure and the voids were
uniformly distributed throughout the oxide at the oxide/metal interface.

34
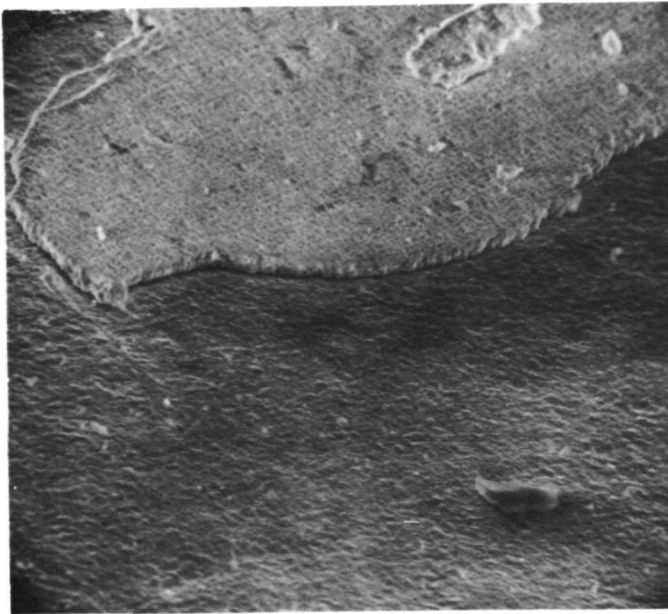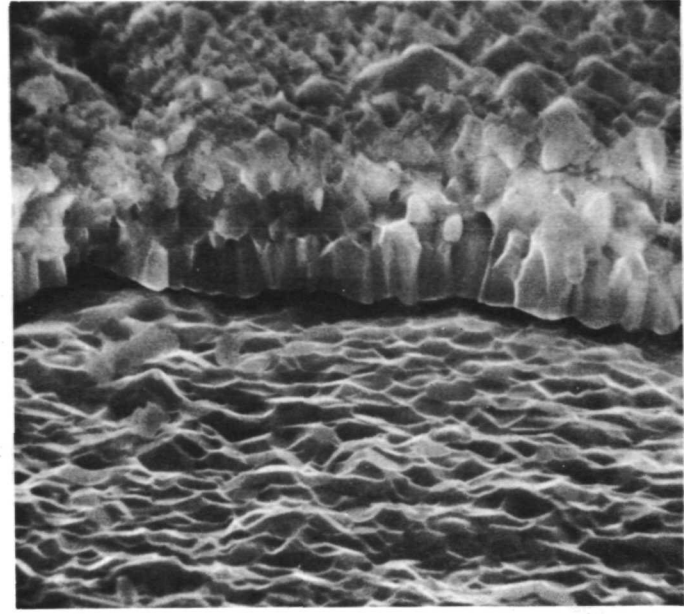
(a)   350X   (b)   3500X
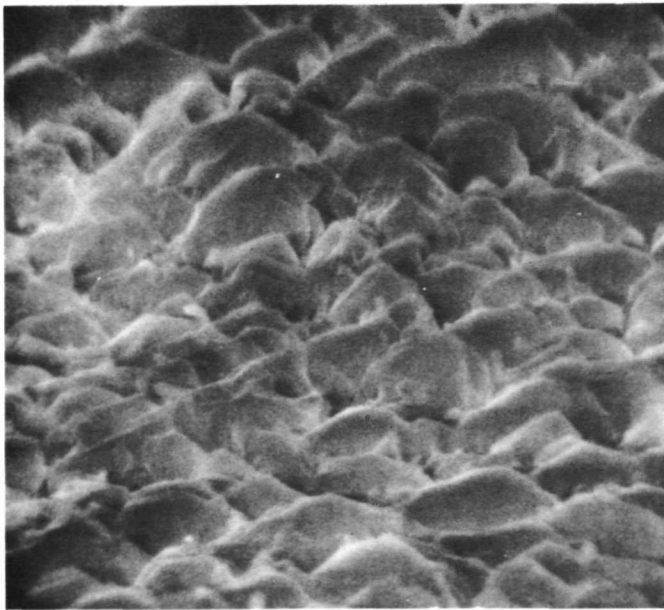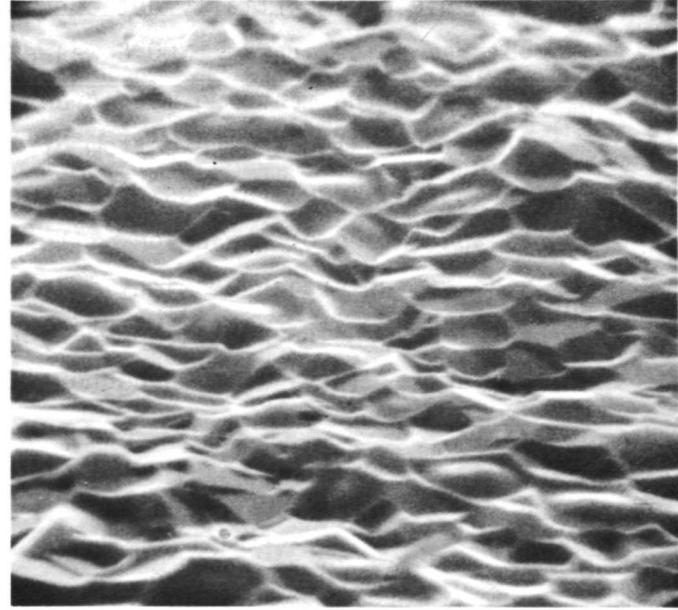
(c)   7500X   (d)   7500X

Fig. 24 Scanning electron micrographs of the partially adherent oxide
scale formed on Ni-10Cr-5Aℓ after 24 hr. of oxidation in air at
1200°C. In (a) a patch of oxide is shown which did not spall on
cooling. Also, the columnar grains of α-Aℓ$_2$O$_3$ can be seen next
to the substrate. (b) is an enlarged view of (a). (c) and (d)
show a more enlarged view of the oxide surface and the substrate
surface, respectively. All the micrographs are taken at 75° tilt.

Voids→

Apparent oxide
thickness at 75°
tilt.

←oxide/metal interface

1700X
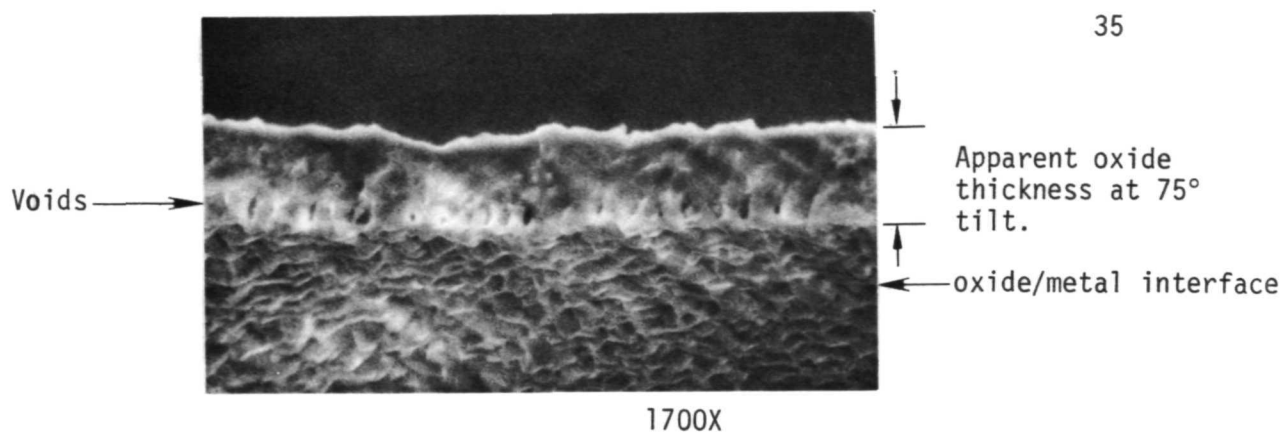
Fig. 25 Scanning electron micrograph of partially spalled Al_2O_3 film after
50 hrs. oxidation of Ni-10Cr-5Al at 1200°C, observed at an angle of
75°. Typical morphology of the oxide/metal interface is shown at
the bottom of the micrograph. A string of voids can be observed
at the oxide/metal interface.
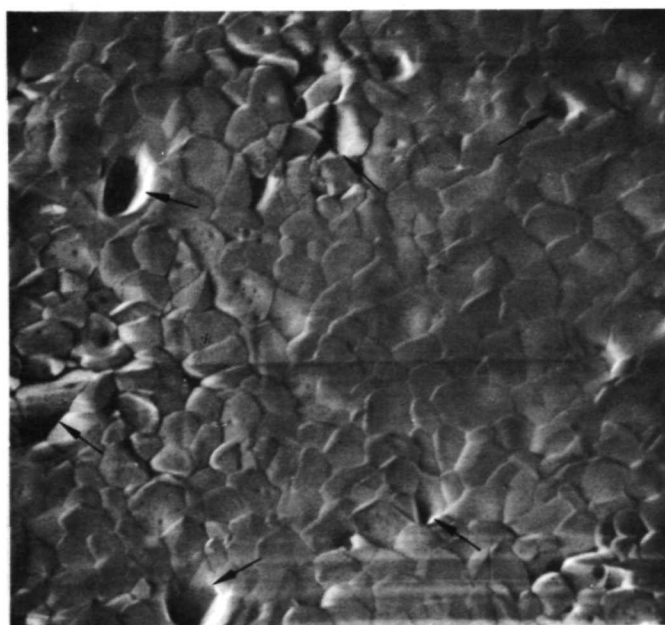
3500X

Fig. 26 Scanning electron micrograph of the bottom of the non-adherent
oxide at the oxide/metal interface, detached from Ni-10Cr-5Al after
50 hrs. oxidation at 1200°C. The granular appearance of the oxide
can be seen. The arrows point at the voids which are always observed.

DISCUSSION

The oxidation mechanism of Ni-Cr-Aℓ ternary alloys is complex and depends upon the composition of the alloy as well as the time, oxygen pressure, and temperature of oxidation. During the preliminary experiments on various Ni-Cr-Aℓ ternary alloys, it was found that a minimum aluminum content of about 5% was required to form a continuous film of $Aℓ_2O_3$ which was by far more protective than a film of Cr_2O_3. However, chromium seems to affect the minimum aluminum content as may be noted from the erratic results obtained on the Ni-5Cr-5Aℓ alloy. A higher chromium content, e.g., 10%, while maintaining the same aluminum content, i.e., 5%, eliminates this problem. Thus, all the studies were made on alloys based on the Ni-10Cr-5Aℓ composition. The only alloy that did not spall was the Ni-12Cr-3Aℓ alloy, which is actually a Cr_2O_3 scale former.

Oxidation of Ni-10Cr-5Aℓ

The oxidation mechanism of the Ni-10Cr-5Aℓ alloy can be described as follows. Upon exposure to air at temperature, NiO nucleated and grew very rapidly by outward nickel diffusion. As NiO formed, the substrate become richer in Aℓ and Cr and subsequently α-$Aℓ_2O_3$ and/or Cr_2O_3 formed. A very small amount of $NiCr_2O_4$ was also detected initially. However, because Cr_2O_3 oxidizes to gaseous CrO_3 at very high temperatures (1100-1200°C), Cr_2O_3 was lost if it was exposed to the oxidant, and thus it was not detected at a later stage. Once a sufficiently thick layer of α-$Aℓ_2O_3$ had formed, the outward diffusion of nickel was inhibited and further formation of NiO ceased. The NiO and α-$Aℓ_2O_3$ formed $NiAℓ_2O_4$ via a solid-state reaction. After extended times, no NiO was detected, and the oxide layer consisted of an outer $NiAℓ_2O_4$ and an inner α-$Aℓ_2O_3$ layer.

The Arrhenius plot for Ni-10Cr-5Aℓ shows a continuously decreasing slope (Fig. 13). Since more than one oxide was present, no physical interpretation can be associated with the activation energies obtained from the Arrhenius plots. However, the amount of α-$Aℓ_2O_3$ and $NiAℓ_2O_4$ increased while the amount of NiO decreased with an increase in temperature and vice-versa (Table I). However, the activation energy obtained for the
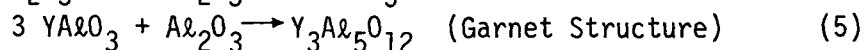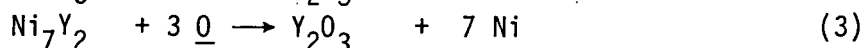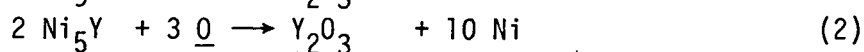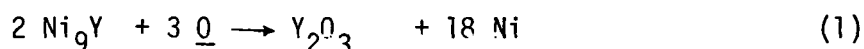
growth of α-$A\ell_2O_3$ by quantitative X-ray diffraction, 50 Kcal/mol, is
valid and can give an insight into the oxidation mechanism. Oishi and
Kingery [11] obtained an activation energy of 152 Kcal/mol for the diffusion
of oxygen in α-$A\ell_2O_3$ above 1600°C, while below 1600°C the activation energy
was only 57.6 Kcal/mol. This change was attributed to the fact that at
lower temperatures the oxygen diffusion rate in α-$A\ell_2O_3$ is structure
sensitive, i.e., oxygen diffusion along the grain boundaries predominates.
Thus, the observed activation energy value of 50 Kcal/mol for the growth
of the alumina scale suggests that oxidation occurred by oxygen diffusion
in the alumina grain boundaries. Because the oxide scale consists of an
outer $NiA\ell_2O_4$ and an inner α-$A\ell_2O_3$ layer at 1200°C, rapid oxygen diffusion
or permeation through $NiA\ell_2O_4$ will cause the oxidation kinetics to be
controlled by oxygen diffusion through the inner α-$A\ell_2O_3$ layer. The
growth of the α-$A\ell_2O_3$ layer was parabolic (Fig. 15), which is attributable
to a diffusion-controlled process, thus this hypothesis is reasonable.

Effect of Yttrium

There was little change in the oxidation kinetics upon the addition
of yttrium to the alumina-former alloy (Ni-10Cr-5Aℓ); however, a large
decrease in the oxidation rate occurred by the addition of yttrium to the
Cr_2O_3 former alloy (Ni-12Cr-3Aℓ). This effect may be due to the formation
of mixed yttrium-aluminum double oxides ($YA\ell O_3$ and $Y_3A\ell_5O_{12}$) which were
detected in small amounts by X-ray diffraction. The double oxides were
present as discrete particles (mostly at the grain boundaries) and not as
a continuous layer. These particles may provide a small, but additional
barrier to the diffusing species and thereby reduce the oxidation rate.
Such oxides were also detected on the alumina-former alloys. It appears
that the protectiveness offered by the mixed oxides is comparable to that
offered by $A\ell_2O_3$.

The activation energy obtained for the oxidation of Ni-10Cr-5Aℓ-0.5Y was
the same (50 Kcal/mol) as for the base alloy, Ni-10Cr-5Aℓ (Fig. 13) which
indicates that the oxidation mechanism was not changed appreciably by the
addition of yttrium. However, the amount of $NiA\ell_2O_4$ formed on the alloy
containing yttrium was greater than on the alloy without yttrium. The
enhanced formation of $NiA\ell_2O_4$ during the oxidation of yttrium-containing

alloys can be explained as follows: The yttrium exists primarily as Ni-Y
intermetallic compounds (Ni_9Y, Ni_5Y, and Ni_7Y_2) in the grain boundaries
of the alloy. A small amount also exists within the grains. Oxidation
of the intermetallic phases results in the formation of Y_2O_3 and metallic
nickel, which subsequently reacts to form NiO. A further reaction occurs
between the NiO and α-Al_2O_3 to form $NiAl_2O_4$. The Y_2O_3 also reacts with
α-Al_2O_3 to form $YAlO_3$ initially and ultimately to form $Y_3Al_5O_{12}$. The
sequence of oxide formation in the presence of yttrium is shown in Fig. 14,
and can be described by the following equations:

$$2\ Ni_9Y + 3\ \underline{0} \longrightarrow Y_2O_3 + 18\ Ni \tag{1}$$
$$2\ Ni_5Y + 3\ \underline{0} \longrightarrow Y_2O_3 + 10\ Ni \tag{2}$$
$$Ni_7Y_2 + 3\ \underline{0} \longrightarrow Y_2O_3 + 7\ Ni \tag{3}$$
$$Y_2O_3 + Al_2O_3 \longrightarrow 2\ YAlO_3 \tag{4}$$
$$3\ YAlO_3 + Al_2O_3 \longrightarrow Y_3Al_5O_{12}\ \text{(Garnet Structure)} \tag{5}$$

The addition of yttrium to Ni-10Cr-5Al caused a slight decrease in
the oxidation rate. Such a reduction in the oxidation rate by the addi-
tion of Y^{3+} to Al_2O_3 cannot be explained by the Wagner-Hauffe theory
because the valences are identical, e.g., trivalent. It is possible,
however, that yttrium can increase the enthalpy of vacancy formation in
α-Al_2O_3 and thus reduce the oxidation rate. The reduction in the oxida-
tion rate may also be attributed to the protectiveness of the yttrium-
aluminum double oxides. The addition of yttrium to alumina scale-formers
virtually eliminated short-term spalling of the scale during cooling.

Effect of Thorium

The activation energy for the oxidation of both Ni-10Cr-5Al-0.5Th and
Ni-10Cr-5Al-1Th was approximately 50 Kcal/mol (Fig. 13). Thus thorium
had virtually no effect on the oxidation mechanism of Ni-10Cr-5Al. However,
the addition of thorium increased the oxidation rate of Ni-10Cr-5Al slightly.
The increase in the oxidation rate by the thorium addition may be due to
a doping effect, because thorium has a valency of 4 (higher than that of
Al) and Al_2O_3 is a p-type semiconductor at 1 atm. air.[12] If this is true,
according to the Wagner-Hauffe theory of doping, Th^{4+} should increase the
oxidation rate.

Thorium additions of 0.5 and 1 w/o to Ni-10Cr-5Aℓ also improved the short-term oxide scale adherence. Thorium and yttrium can be expected to prove similar effects as both of them are chemically similar.

The quaternary addition of thorium formed only its own oxide, i.e., ThO_2 particles; no double oxide of thorium formed, as in the case of yttrium-containing alloys.

Oxide Scale Adherence

It has already been noted that the oxide on Ni-10Cr-5Aℓ spalled readily upon cooling even after 15 min. of oxidation at 1200°C. Both yttrium and thorium markedly improved the short-term scale adherence. Although the long-term spalling resistance (after one week of oxidation at 1200°C) was improved somewhat, e.g., the scale did not spall off completely, some spalling did occur. Thorium appears to be a better addition than yttrium in terms of oxide-scale adherence. This behavior can be attributed to the fact that thoria does not form double oxides with alumina as does yttria. There is a much greater volume expansion, resulting in mechanical stresses, when YAG forms compared to that associated with the formation of ThO_2 particles. This was confirmed by the observation that the onset of spalling was associated with the appearance of the YAG particles after oxidation of the Ni-10Cr-5Aℓ-0.5Y alloy at 1200°C in air for 200 mins. (Fig. 14), as compared with the alloy containing thorium which did not spall for about one week under the same conditions. The YAG and ThO_2 particles act as stress-raisers and literally push the oxide layer away from the substrate. This results in the fracture of the oxide and subsequently causes spalling.

The tremendous improvement in the oxide-scale adherence with small additions of yttrium or thorium cannot be explained on the basis of most of the factors commonly proposed for the improvement of oxide-scale adherence, such as a reduction in the Pilling-Bedworth ratio, improved oxide-film plasticity, or a decrease in the difference between the thermal expansion coefficients of the oxide and the substrate. The "oxide-pegging" mechanism, or what is commonly known as the "key-on effect," can also be precluded since no oxide pegs were observed at the oxide/alloy interface (Figs. 16 and 17). It was therefore concluded that the presence

of voids at the alloy/oxide interface may play an important role in spalling. A similar mechanism has been observed by Tien and Rand,[13] and Tien and Pettit[14] on Ni-12Al and Fe-25Cr-4Al, respectively, both of the alloys being alumina formers at 1200°C.

Voids were observed at the alloy/oxide interface as shown by the scanning electron micrographs in Figs. 25 and 26 on Ni-10Cr-5Al after oxidation at 1200°C for 50 hrs. In contrast, no voids at the alloy/oxide interface were observed on the alloys containing thorium and yttrium, Figs. 20 and 22, respectively. Based upon these observations a model is proposed similar to that of Tien and Rand,[13] and Tien and Pettit,[14] which explains the improvement of the oxide-scale adherence on alloys containing yttrium and thorium.

As described earlier, for the Ni-10Cr-5Al alloy, once the outer $NiAl_2O_4$ layer is separated from the substrate by the intervening $\alpha\text{-}Al_2O_3$ layer, the $\alpha\text{-}Al_2O_3$ scale grows by inward diffusion of oxygen along the grain boundaries. This mechanism of oxidation was suggested on the basis of the value of the activation energy of 50 Kcal/mol. The voids observed at the alloy/oxide interface are Kirkendall voids which form first in the substrate due to outward nickel diffusion and thereafter due to the selective oxidation of aluminum. The vacancies are formed by unequal diffusion of Al atoms towards the external oxide scale and back diffusion of Ni and Cr atoms in the opposite direction. Initially the voids are formed within the substrate near the alloy/oxide interface, but eventually are incorporated into the alloy/oxide interface because inward growth of the $\alpha\text{-}Al_2O_3$ occurs consuming the substrate. Furthermore, since the diffusion of aluminum to the oxide and diffusion of other atoms into the alloy takes place from the void/substrate interface, the voids also move inwards along with the oxide/alloy interface, and thus the voids are never completely enveloped within the oxide scale. The voids also keep on growing by the precipitation of additional vacancies as the oxidation process continues. The failure of the scale occurs at the alloy/oxide interface due to the presence of a large number of these voids which act as stress concentration sites.

Rare-earth oxide particles such as Y_2O_3, $Y_3Al_5O_{12}$, and ThO_2 act as vacancy sinks at sites away from the alloy/oxide interface, thus preventing

void formation and improving the oxide-scale adherence. Yttrium and thorium can also provide vacancy-sinks by forming complexes with the vacancies.[14] Since the atoms of Y and Th are large as compared to the base alloy atoms, i.e., Ni, Cr, and Aℓ, the dilatational strain energy associated with the larger atoms can be decreased if these atoms form atom-vacancy complexes with the excess vacancies. This "vacancy-sink" mechanism can explain why none or very few voids are observed at the alloy/oxide interface in the presence of yttrium and thorium, thus improving the oxide-scale adherence.

REFERENCES

1. Douglass, D.L., Proc. 1971 Conference of Society of Aerospace Materials and Process Engineers 16 (1971) 1.

2. Douglass, D.L. and Armijo, J.S., Oxidation of Metals 2 (1970) 207.

3. Pettit, F.S., Trans. AIME 239 (1967) 1296.

4. Wallwork, G.R. and Hed, A.Z., Oxidation of Metals 3 (1971) 171.

5. Kvernes, I. and Kofstad, P., "Studies on the Behavior of Nickel-Base Superalloys at High Temperatures," Tech. Report AFML-TR-70-103, July 1970.

6. Scott, F.H. and Wood, G.C., Corr. Science 11 (1971) 799.

7. Kosak, R, Ph.D. Thesis, The Ohio State University (1969).

8. Santoro, G.J., Deadmore, D.L., and Lowell, C.E., "Oxidation of Alloys in the Ni-Aℓ System with Third Element Additions of Cr, Si, and Ti at 1100°C," NASA-TN-D-6414, July 1971.

9. Taylor, A., and Hinton, K.G., J. Inst. of Metals 81 (1952-53) 169.

10. Taylor, A., and Floyd, R.W., J. Inst. of Metals 81 (1952-53) 451.

11. Oishi, Y., and Kingery, Jr., W.D., J. Chem. Physics 38 (1960) 480.

12. Pappis, J., and Kingery, W.D., J. Amer. Ceramic Soc. 44 (1961) 459.

13. Tien, J.K., and Rand, W.H., Scripta Met. 6 (1972) 55.

14. Tien, J.K. and Pettit, F.S., Met. Trans. 3 (1972) 1587.

Page Intentionally Left Blank

"The aeronautical and space activities of the United States shall be conducted so as to contribute . . . to the expansion of human knowledge of phenomena in the atmosphere and space. The Administration shall provide for the widest practicable and appropriate dissemination of information concerning its activities and the results thereof."

—NATIONAL AERONAUTICS AND SPACE ACT OF 1958

NASA SCIENTIFIC AND TECHNICAL PUBLICATIONS

TECHNICAL REPORTS: Scientific and technical information considered important, complete, and a lasting contribution to existing knowledge.

TECHNICAL NOTES: Information less broad in scope but nevertheless of importance as a contribution to existing knowledge.

TECHNICAL MEMORANDUMS: Information receiving limited distribution because of preliminary data, security classification, or other reasons. Also includes conference proceedings with either limited or unlimited distribution.

CONTRACTOR REPORTS: Scientific and technical information generated under a NASA contract or grant and considered an important contribution to existing knowledge.

TECHNICAL TRANSLATIONS: Information published in a foreign language considered to merit NASA distribution in English.

SPECIAL PUBLICATIONS: Information derived from or of value to NASA activities. Publications include final reports of major projects, monographs, data compilations, handbooks, sourcebooks, and special bibliographies.

TECHNOLOGY UTILIZATION PUBLICATIONS: Information on technology used by NASA that may be of particular interest in commercial and other non-aerospace applications. Publications include Tech Briefs, Technology Utilization Reports and Technology Surveys.

Details on the availability of these publications may be obtained from:

SCIENTIFIC AND TECHNICAL INFORMATION OFFICE

NATIONAL AERONAUTICS AND SPACE ADMINISTRATION
Washington, D.C. 20546